ChemCatChem

Review
doi.org/10.1002/cctc.202300961

Chemistry Europe
European Chemical Societies Publishing

www.chemcatchem.org

Eco-sustainable Synthesis of *N*-containing Heterocyclic Systems Using Porous Carbon Catalysts

Elena Pérez-Mayoral,*[a] Marina Godino-Ojer,[b] Luisa M. Pastrana-Martínez,[c] Sergio Morales-Torres,[c] and Francisco J. Maldonado-Hódar*[c]

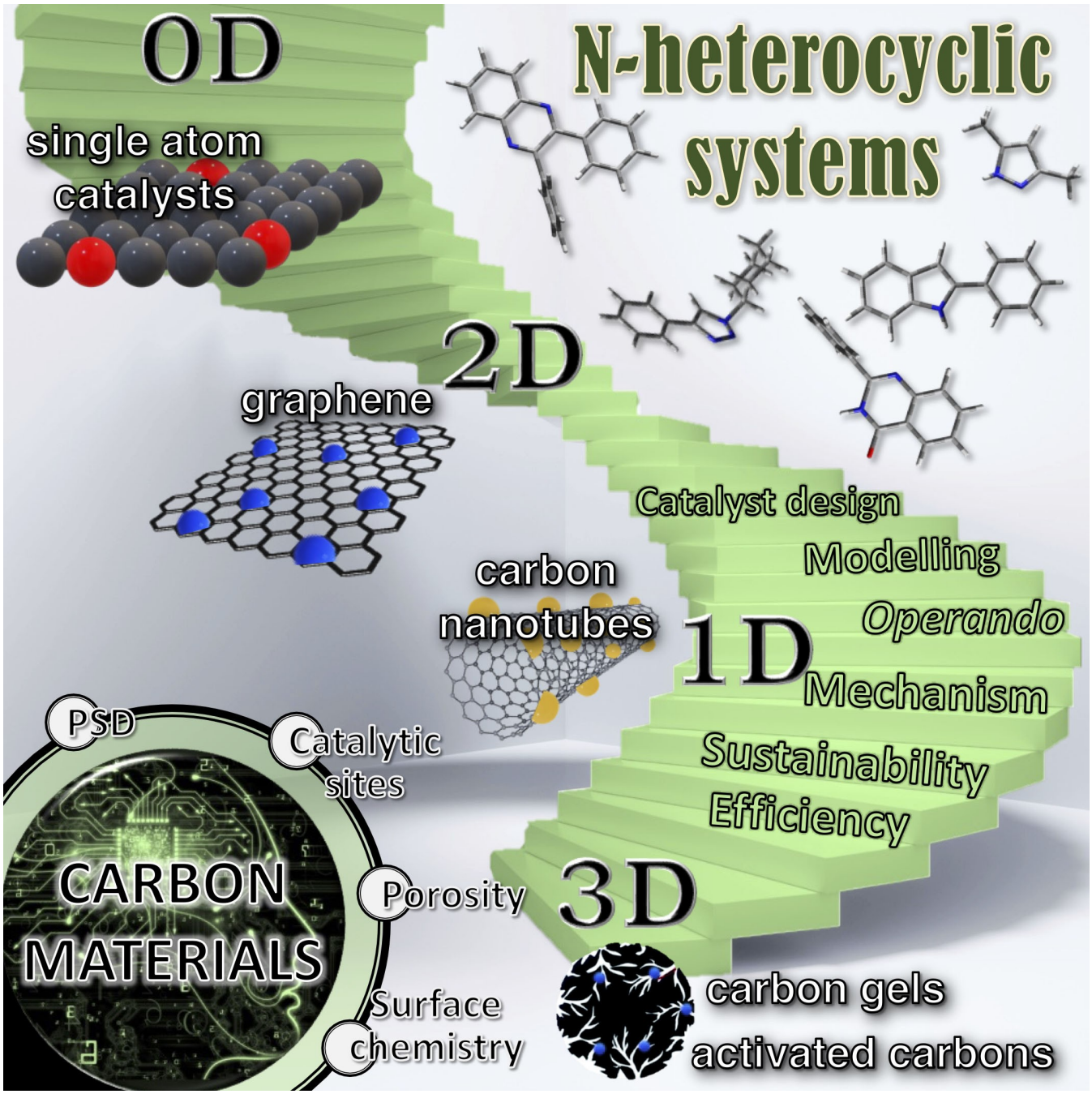

From the most classic carbon materials (CMs) to the advanced ones, all of them integrate a promising catalyst set in terms of sustainability and energy efficiency for a greener future. Different synthetic strategies concerning to the catalytic synthesis of relevant *N*-containing heterocycles are herein described to address the great potential of the referred catalysts flying over what has been done and all that remains to be done. Current trends in this field involve structure-activity relationships establishment also considering the reaction mechanisms understanding and the identification of active catalytic sites, as function of both experimental datasets, emphasizing on operando characterization techniques, and theoretical studies which will significantly contribute to the design of custom-made catalysts as a new horizon.

1. Introduction

Heterogeneous catalysis plays an indubitable role in the sustainable development of society, allowing saving both reactants and energy; a wide range of materials with a very diverse nature and structure currently catalyzes around 98% of the production processes.

Among them, carbon materials (CMs) are not the most popular type of materials used in catalysis, because the formation of carbon deposits or coke from hydrocarbons is one of the main cause of catalysts deactivation, many processes being forced to enhance the catalytic activity or selectivity of different catalysts.[1]

The limitations of CMs are typically associated to their combustible character since they may be burned out in an oxidant atmosphere at high temperatures. However, this drawback also becomes an advantage when it comes to recovering supported active phases from spent catalysts, specifically expensive noble metals (Pt, Au, Pd, etc) by simple calcination of the carbonaceous support. In contrast, CMs are stable in processes carried out under inert atmosphere even at high temperatures (do not easily undergo sintering or phase changes) and are also stable in strong acid or basic solutions.

The advantages of CMs as catalysts or catalyst supports were highlighted in the literature over the years,[2] and continuously improved by the progressive development of novel forms of carbon nanomaterials.[3] These advantages are often related to the versatility of their physico-chemical properties – porosity, surface chemistry –, which are easily tuned by activation or functionalization treatments,[4] high competitiveness (low manufacture price) and availability, because they can be synthesized in different formats – powder, pellets, grain, thin coatings, foams, fibers and fabrics, etc. – from many different precursors, including cheap wastes or biomass.

Nowadays, there is a wide variety of CMs (Figure 1) with very different morphology, porosity and surface chemistry, tailored at the macro- and nanoscale, which motivates the selection of the best material for each application, even adjusted to the reactor characteristics. Franklin[5] stablished the first classification of CMs categorized into graphitic and non-graphitic ones, the latter materials being also divided into graphitizing and non-graphitizing. Another classification is to define the three "classic" allotropes of carbon – diamond, sp^3, graphite, sp^2, and carbine, sp –, and their derivatives.[6] This versatile hybridization of carbon allows the formation of different amorphous or crystalline structures. In fact, CMs are also classified in different subgroups according to their shape and dimensions,[7] from 0D molecules of fullerenes and quantum dots (CDs <10 nm), 1D carbon nanotubes (CNTs) or nanofibers (CNFs), 2D graphenes or carbon nitrides (C_3N_4), to 3D carbon foams, carbon gels or the classic activated carbons (ACs).

Heterocycles are a type of organic compounds often present in a great variety of natural products and pharmaceuticals. These compounds are extremely relevant in life science,

[a] *Prof. E. Pérez-Mayoral*
Departamento Química Inorgánica y Química Técnica
Facultad de Ciencias
Universidad Nacional de Educación a Distancia, UNED
Urbanización Monte Rozas, Avda. Esparta s/n Ctra. de Las Rozas al Escorial Km 5, 28232 Las Rozas, Madrid (Spain)
E-mail: eperez@ccia.uned.es

[b] *Dr. M. Godino-Ojer*
Facultad de Ciencias Experimentales
Universidad Francisco de Vitoria, UFV
Ctra. Pozuelo-Majadahonda 8 km 1.800, 28223 Pozuelo de Alarcón, Madrid (Spain)

[c] *Dr. L. M. Pastrana-Martínez, S. Morales-Torres, F. J. Maldonado-Hódar*
NanoTech – Nanomaterials and Sustainable Chemical Technologies
Departamento de Química Inorgánica
Facultad de Ciencias
Universidad de Granada, UGR
Avenida de Fuente Nueva, 18071 Granada (Spain)
E-mail: fjmaldon@ugr.es

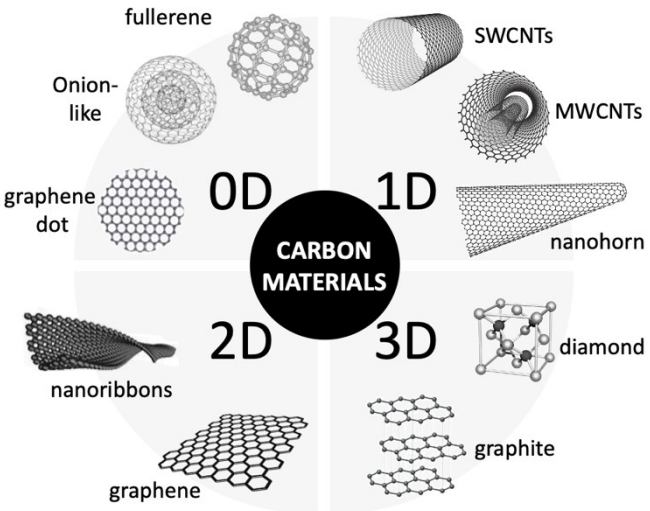

Figure 1. Classification of CMs.

being part of naturally occurring products such as, alkaloids, vitamins, hormones, nucleic acids, enzymes and co-enzymes and antibiotics, among others. Figure 2 shows some biologically active heterocycles including natural products and traditional pharmaceuticals or approved prescribed drugs.

Heterocyclic systems are also applied in multiple researching fields such as nanochemistry, molecular devices and sensors, combinatorial and supramolecular chemistry, catalysis and others.[8] In addition, some of these compounds comprise an important type of ionic liquids (ILs) acting as green solvents or even as catalysts frequently used by pharmaceutical industry.[9] Even so, some porous materials are also built from

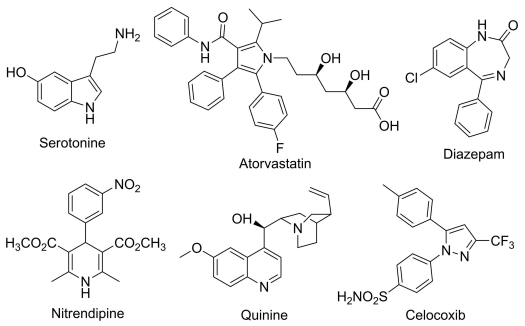

Figure 2. Pharmacologically relevant nitrogen-containing heterocycles.

E. Pérez-Mayoral is Full Professor at the National Education University at the Distance, UNED (Spain), in Science Faculty, since 2022 with docent activity in different degree, master and doctorate programs in chemistry and environmental sciences. She has worked in different research fields, including organic photochemistry, medicinal chemistry and heterogeneous catalysis for fine chemical synthesis. Her current research interests are focused on the design of new nanocatalysts involved in the green synthesis of relevant heterocycles and reaction mechanisms understanding by using computational methods. She is co-authored of 92 publications, 9 patents and more than 140 communications in national and international conferences.

M. Godino-Ojer is Associate Professor at the Francisco de Vitoria University (Madrid, Spain) since 2021. She obtained her PhD in 2017 at the National Education University at the Distance (Departement of Inorganic Chemistry and Technical Chemistry). Her research interests focus on the sustainable chemistry, synthesis of bioactive heterocycles, heterogeneous catalysis and, application of theoretical calculations to the study of reaction mechanisms. To date, she is co-authored of a patent, 25 publications and more than 55 communications in international congresses. She is regularly involved in activities promoting the scientific knowledge at all academic levels.

L. M. Pastrana-Martínez is graduated in Chemistry by the University of Jaén (Spain) and received the Ph.D diploma at the same institution in June 2010. She is Associate Professor at the University of Granada since 2023. Her main research interests are focused on environmentally friendly technologies for management and treatment of air and water using nano- structured materials. Her scientific research output included more than 72 scientific papers, 7 book chapters and more than 120 communications in national and international conferences. She has been involved in more than 23 funded national and international projects and 6 as principal investigator.

S. Morales Torres is Associate Researcher at Faculty of Sciences of University of Granada (Spain) since 2017. He received a PhD degree in Chemistry from UGR in 2009 and then, he did a postdoctoral stage at Faculty of Engineering - University of Porto (Portugal) for 7 years. His research interest involves the development of carbon nanostructures, catalysts and membranes for energy and environmental applications. To date, he co-authored a patent, 75 articles in international JCR journals and 12 book chapters. He acted as guest Editor of 5 special issues of international scientific journals and supervised several PhD and undergraduate students.

F. J. Maldonado-Hódar is Full Professor at the University of Granada (Department of Inorganic Chemistry) since 2012 with docent activities in various degrees, Doctorate and Master Programs, as well Specialization Courses in the field of Heterogeneous Catalysis and Material Sciences. His research is focused on the design of advanced nanomaterials and the study of their applications through adsorption and catalysis for the production of clean energy, valuable products from fine chemistry or environmental processes for the air and water protection. Is co-author of 6 International patents, more than 160 publications cited around 7000 times (h = 42), 8 books chapters, more than 200 communications in International Congresses.

heterocyclic scaffolds, zeolites and metal-organic framework (MOFs), among them.[10]

Sustainable Development Goals (SDGs) integrate relevant chemistry challenges opening opportunities for new, green and sustainable chemical research and practices. In this context, CMs represent an opportunity in the optimization of clean and sustainable production processes. Cleaner production, preventing the production of wastes, but improving the efficiency of the energy, water and resources, among others, is essential to protect the planet, the societies becoming more sustainable. In general, CMs have been extensively applied in fine chemical synthesis, metal-supported carbon catalysts derived from ACs being protagonists in both industry and academia, mainly due to economic reasons.[11] In fact, BASF is a leader company in providing catalytic technologies useful in the pharmaceutical and fine chemical industry; heterogeneous precious-metal catalysts such as Pd, Pt, Rh, Ru, etc., being dispersed on CMs and other inorganic supports, as some examples. Much more recently, the development of advanced functional porous carbons, prepared from direct pyrolysis of MOFs or covalent organic frameworks (COFs), in the presence or not of others carbon or heteroatom sources, have acquired a relevant attention.[12] In this context, the development of highly dispersed metal-supported heteroatom-doped carbon catalysts or even, single-atom carbon catalysts (SACs), in which isolated metal atoms at sub-nanometer scale are distributed at the carbon surface, is a hot topic. Both MOFs and COFs have been reported as ideal platforms to develop SACs, an area in expansion representing a new frontier, particularly in heterogeneous catalysis. These CMs show higher thermal stability compared to their precursors and enhanced porosity, which in conjunction to their adjustable and uniform dopant distribution, and in some cases the presence of metal phases atomically dispersed, contribute to enhance the catalytic performance.[12b,13]

The aim of this manuscript is not to make a detailed review of all types of CMs, their composites, or catalyst derivatives, but to establish an overview of the relationship between their properties and the catalytic behavior in the synthesis of valuable compounds, specifically nitrogen-containing heterocyclic systems. More specifically, subsequent sections represent an overview concerning the general characteristics and practical synthetic approaches to prepare the most relevant CMs, applied to the synthesis of heterocyclic systems by following the synthetic strategy of building the heterocyclic core.

2. Carbon Materials: Synthesis, and General Characteristics

It is well-known that all factors favoring the accessibility of molecules or reactants to active catalytic sites greatly influence on the catalytic performance. Thus, porosity, metal content, dispersion, and location of metal nanoparticles at the surface are keys for catalyst design.[14]

The properties of CMs are history-dependent, i.e., strongly related with the precursors and experimental conditions used on the different synthesis procedures (Table 1). The reactivity of CMs depends on the nature, concentration, and distribution (accessibility) of active sites through the pore size distribution (PSD). Active sites are in general, associated to the edges, basal plane defects, heteroatoms (O, N, S, P) or metallic active sites from natural inorganic impurities of raw materials.[15] The developed porosity and the possibility to generate specific anchoring sites for active phases also stablish that CMs are excellent candidates to prepare supported catalysts or even composite materials, thus generating additional metallic active sites. Once again, the characteristics – chemical and crystalline phase, dispersion and distribution, etc. – of these active phases, and consequently, the performance of these supported catalysts, are strongly dependent on the treatment conditions.[16]

2.1. Activated carbons (ACs)

ACs are classical porous materials prepared from very different precursors as petroleum coke, coals, peats, sewage sludge, manure or lignocellulosic precursors as woods, coconut shells, fruit stones or discarded plastics.[17] These high carbon content

Table 1. Summary of the main properties of the most used CMs in catalysis.

CM	Synthesis	Porosity	Surface chemistry	Other
Activated carbons	Pyrolysis, physical/ chemical actions	Very high S_{BET} and W_0	Basic/acid nature strongly dependent of the activation degree and procedure. Easy chemical functionalization	Cheap manufacture from wastes and biomass
CNTs	Electric arc discharge, laser ablation, CVD	Low-middle S_{BET} and W_0. High S_{EXT} and V_2	Low heteroatom contents, but typically present metal residues. Neutral/ hydrophobic nature. Medium-difficult chemical functionalization	High electric, thermal and mechanical properties
Graphene derivatives	CVD, chemical exfoliation, chemical synthesis, mechanical cleaving	Low-middle S_{BET}. Porosity depending on the sheet staking	Oxygen content dependent of some synthesis procedures (GO + reduction). Medium-difficult chemical functionalization	Excellent electrical conductivity and strong mechanical and thermal strength
Carbon gels	Sol-gel method, pyrolysis/activation methods	Middle-high S_{BET} and W_0. High V_2 and V_3	Fitted according to the monomer selected and thermal treatments. Easy chemical functionalization	Purity, tunable porosity at nanoscale

S_{BET} = Brunauer, Emmett and Teller surface area; S_{EXT} = External surface area; W_0 = micropore volume; V_2 = mesopore volume; V_3 = macropore volume.

raw materials are treated by chemical and physical activations to remove volatile matter, allowing the formation of micro-, meso- or macropores. The porosity is generated from the random disposition of graphenic layers (sp^2) between amorphous carbon (sp^3) in the so-called "turbostratic carbon structure". Physical activation is typically carried out in two steps: (i) pyrolysis under an inert atmosphere and (ii) sequential gasification by reaction with steam, CO_2 or oxygen flow. On the other hand, the chemical activation requires the preparation of mixtures between the raw materials and activating agents such as NaOH, KOH, K_2CO_3, H_3PO_4 or $ZnCl_2$. Raw materials can be also previously carbonized in a separate step and then, the corresponding char being activated later under a two-step activation. The activation occurs during a posterior thermal treatment in inert atmosphere by reaction between both components leading to the development of the porous structure. Finally, samples should be carefully washed to remove impurities and unreacted agents. Depending on the precursors and the synthesis parameters, the activation degree can be fitted to determine the porosity degree and PSD. Consequently, the optimization of production route and process conditions are need for the synthesis of ACs, as well as the modelling through experimental design tools saves time and resources.[18]

The activation degree does not only affect on the porosity but also parameters such as the graphitic character, the heteroatoms or inorganic contents, thus influencing on characteristics such as conductivity, hydrophilicity or acid/basic character of the surfaces, and consequently the interactions with reactants or with the supported active phases. The importance of the surface chemistry of ACs in catalysis is also well-known.[19] Thus, as-prepared ACs can be subsequently modified by secondary treatments to induce different chemical functionalities, mainly those containing oxygen (O), nitrogen (N), sulfur (S), halogens, boron (B) or phosphorus (P) groups, by oxidation,[20] halogenation,[21] nitridation[22] etc., but also by impregnation, chemical vapor deposition (CVD), hydrothermal treatments or dry-milling, typically combined with heat treatments. In fact, these treatments of activation and/or functionalization are common for all CMs.

ACs are widely used as adsorbents or molecular sieves in drinking water treatment, air filtration, purification and separation of gases, wastewater treatment, and different treatments of the food industry. In catalysis, ACs behave as an excellent support of catalytic nanoparticles and are largely used in industrial, particularly in selective hydrogenation reactions. The market for ACs is on the rise, although it still needs to take into account the principles of the bioeconomy and circular economy,[23] the use of waste or biomass,[17] and the environmental implications related to manufacturing and use through a life cycle impact assessment.[24]

2.2. Nanostructured carbon materials

The exponential increase of the investigations on the synthesis of novel carbon nanostructures have significantly extended the types of CMs suitable for catalytic applications. Thus, it is important to outline the general trends and perspectives in this dynamic research field.

2.2.1. 1D-CNTs and CNFs

Although CNTs were described earlier, Ijima's works[25] marks the roadmap of the huge development of CNT-based technologies. The production of CNTs at large scale promotes the application of CNTs in diverse fields. The methods of CNT synthesis using graphite as precursor mainly involve laser or plasma-based method (arc discharge), but a huge amount of energy is required. Alternatively, CVD from ethylene or acetylene produces multi-walled carbon nanotubes (MWCNTs) at large scale and a reasonable cost.[26] The dimensions, external and internal diameter, of CNTs depend on the synthesis conditions – metal dispersion, temperature, reaction time, etc – .[27] The main limitations to its extensive use are associated with the presence of impurities, the lack of morphological or structural uniformity, length and chirality, and the tendency of CNTs to bundling, which hinders the permeation and diffusion of gases.

Structurally, CNTs may be defined as graphene sheets rolled into cylindrical shapes, and they are differentiated into single-walled carbon nanotubes (SWCNTs) or MWCNTs. In this case, the concentric graphene layers showed a spacing between 0.34 to 0.39 nm, slightly larger than in the crystalline graphite ($d = 0.335$ nm). Their characteristics also differ depending on how the graphene sheets are rolled into "zigzag", "chair", or "chiral" nanotubes. The internal diameters of these nanotubes range from narrow micropores of around 0.7 nm to the mesopore range > 2.0 nm for MWCNTs. Carbon nanofibers (CNFs) are formed when the graphenic layers present a certain curvature (α) regarding the edge of the fibers and are stacked forming different structures.[28] Both CNTs and CNFs are very light materials, with excellent mechanical, electrical and thermal properties, mainly related with the sp^2 nature of the C–C bonds. In addition, they are extensively used to prepare reinforced composite materials due to the high ratio diameter / length. The main problems of both 1D-materials are associated to the nature of their hydrophobic surfaces, decreasing dispersion, and leading to a poor interfacial interaction with water solutions or polymeric matrixes. This is also a drawback to prepare supported catalysts, but it can be overcome by covalent or non-covalent functionalization of the surfaces. Ball milling, treatment with surfactants or wet chemical oxidations with strong oxidants are typically used.[29]

Catalysts prepared using CNTs are divided into supported or confined catalysts, where the active sites are located on the external surface or within the CNT channels. Specific synthesis strategies were developed for both cases.[3c] The interactions of metallic nanoparticles with the inner wall of the nanotube produce the confinement effect, which can modulate the reducibility, sintering or leaching resistance, and in general, lead to more active species.[3c] To obtain the nanoparticles exclusively on the outer surface, closed CNTs are used.

Alternatively, high-boiling organic solvents such as ethylene glycol or xylene are used to temporarily block the CNT channels.[30] The organic solvent prevents the entry of the aqueous solutions of the metal precursors, which when evaporated will leave the metal preferentially on the functional groups of the outer surface. To generate confined nanoparticles within the CNT channels, there are also several approaches. They can be obtained directly during the growth of the nanotube by *in situ* encapsulation method.[31] Alternatively, the deposition of the metals inside the channels by impregnation is evidently more feasible in MWCNTs than in SWCNTs, since the first ones typically have a larger diameter (4–20 nm) than the latter (0.7–2 nm). In fact, the strong diffusional constraints in the micropores limit the production of this type of catalysts using SWCNTs, while capillary forces favor the filling of the mesopores and the adsorption of the precursors inside the MWCNTs.

The surface chemistry of CNTs can be also modified by chemical functionalization, which can be carried out by gas or liquid treatments. Typical gas phase oxidants are oxygen, steam, ozone or carbon dioxide,[32] while the most liquid phase methods include the use of hydrogen peroxide (H_2O_2),[33] ammonium persulfate ($(NH_4)_2S_2O_8$),[34] nitric acid (HNO_3),[34–35] sulfuric acid (H_2SO_4),[36] mixtures of both (HNO_3/H_2SO_4),[37] "piranha" solution (H_2O_2/H_2SO_4)[38] or potassium permanganate ($KMnO_4$).[39] All the oxidation treatments seek to turn CNTs more hydrophilic and soluble in polar solvents, as well as to modify their acid-basic nature, leading to different interactions with the reactant molecules and/or metallic phases during the synthesis of metal-supported catalysts. Nevertheless, in the specific case of CNTs, the creation of oxygenated surface groups (OSGs) on the tube edges and sidewall defects of CNTs lead to other structural effects such as the removal of the metal particles used during the nanotube growth by CVD, the oxidation of amorphous carbon, the modification of CNT bundles (expansion and new bundles), opening of the tube tips and shortening of the tubes, among others,[35b,40] these changes being also depending on the type of CNTs (SWCNTs *vs.* MWCNTs), and even their dimensions (diameters and length).[34]

2.2.2. 2D-Graphene and its derivatives

Since Novoselov and Geim's works in 2004,[41] graphene attracted a great interest for both researchers and engineers. Graphene can be produced by different methods, such as nanotube slicing, CVD, and by exfoliation of graphite, among others. In addition, graphite can be oxidized to graphite oxide by Hummers' or Brodie's methods,[42] among others, which yields to graphene oxide (GO) sheets after mechanical/chemical exfoliation and then, GO can be progressively reduced by thermal and/or chemical treatments to reduced graphene oxide (rGO), which possesses still some OSGs and structural defects, and thereby, should not be confused with pristine graphene.[43] In spite that this method leads to a material with different concentration of defects, the easy and preparation process at large scale, and lower cost, together the potential chemical functionalization – epoxide, hydroxyl, carbonyl and carboxylic acid groups – makes it the most widely synthetic method used.

Ideally, graphene is a single-layer 2D material with sp^2 hybridization between carbons in hexagonal arrangement, being the basic structure of fullerenes (0D), nanotubes (1D) or graphite (3D). This arrangement provides a theoretical exceptional high surface area, conductivity, or mechanical strength. Nevertheless, the OSGs in the GO sheets generate some carbon in sp^3 hybridization, which disrupt the conduction of delocalized π electrons through the basal planes. These OSGs need to be reduced in order to restore the sp^2 network.[44] Similarly, the theoretical specific surface area of completely exfoliated graphene is assumed to be 2620 $m^2 g^{-1}$. However, the surface area of the prepared graphene-based materials calculated by several experimental techniques is rather less. Pristine graphene prefers to interact with hydrophobic molecules, while other graphene derivatives such as GO, strongly interact with polar molecules due to the large amount of OSGs, in particular hydroxyl/epoxide and carboxyl acid groups.[45] The adsorption of aromatic compounds is also favored in rGO regarding GO as consequence of its hydrophobicity and the π–π interactions.

Concerning the metal deposition on graphene sheets, authors consider the binding of the adatoms over graphene sheets on three sites of high symmetry: hollow (H) at the center of a hexagon, bridge (B) at the midpoint of a C–C bond, and top (T) directly above a carbon atom. The adsorption energy for Au, Ag and Cu is low (physisorption), whereas Co, Ni, Pt and Pd are covalently bonded to graphene (chemisorption). The occupation of the adsorption sites depends on the electronic configuration of transition metals. Cu, Pd or Pt, with filled or nearly filled *d*-orbitals being adsorbed on B or T sites, while Fe, Co or Ni prefer H sites.[46]

Although the properties previously exposed show the enormous potential of graphene in catalysis, the low bulk density of graphene induces a very low catalyst mass / reactor volume ratio when use fixed-bed reactors. To solve this problem, it was proposed the macroscopic shaping of graphene powders into pellets by extrusion and more recently, the preparation of porous graphene aerogels.[47]

Noble metals nanoparticles – Pt, Au, Pd, etc – decorating the graphene surface can be obtained by wet impregnation carefully controlling the type of solvent, nature and concentration of metal precursor, surfactants, deposition time or temperature. Functionalization to induce anchoring sites for the metal precursor nucleation favours the covalent bond of the metal to the basal planes of graphene improving the metal dispersions.[48] Graphene-based catalysts can be also obtained by combination of graphene and metal oxides (TiO_2, ZnO, Fe_3O_4, etc) to yield graphene-metal composites.[49] As an example, the GO/TiO_2 composites showed enhanced properties as photocatalysts under visible conditions.[43a] Important advances in photocatalytic materials based on graphene derivatives and their integration in photocatalytic-ultrafiltration systems as photocatalytic membrane reactors using simulated solar light or visible irradiations were obtained from the works of Pastrana-Martínez et al.[49a,50]

2.2.3. 3D Carbon gels

The preparation of porous solids by sol-gel techniques presents different advantages regarding others such as, nanocasting, electrospinning, etc., mainly due to the simplicity of the process allowing to obtain materials in an one-pot procedure.[51] In contrast with silica gels patented in 1919,[52] carbon gels were first developed in the late 1980 s[53] and patented in 1991.[54] Although carbon gels are now being prepared using a wide range of alternative monomers[55] and many others organic precursors, from newspaper[56] to graphene,[47] the original recipe uses the polymerization of resorcinol (R) and formaldehyde (F) catalyzed (C) by soft basis (Na_2CO_3) in aqueous solution (W).[53] The morphology of the R–F polymer (coral-like structure) consists in the 3D-crosslinking of nearly spherical particles (primary particles), where the solvent is retained between them. The size and overlapping degree of these primary particles is determined during the polymerization step, controlled therefore by the reaction conditions: nature, ratio and concentration of reactants (R/F, R/C, R/W), solvents and polymerization catalysts, reaction temperature, time and pH. The reaction mechanism is well stablished.[57] The solvent occupies the porosity between particles, and evidently, the stacking of larger particles leaves wider pores between them; this porosity must be preserved during the drying step to avoid the shrinkage or even, porosity collapse, allowing to generate mainly meso- or macropores. Aerogels, xerogels or cryogels are obtained depending on the drying procedure used.[58] Supercritical drying (to aerogels) preserves the porosity in a greater degree, but the technical application makes difficult at a large-scale synthesis. Similarly, cryogenic method generates macro- and megalopores due to the ice crystal growth, which compromises the mechanical stability of the monolith.[59] Alternative and fast drying procedures (microwave, plasma) to obtain xerogels have been also developed,[60] samples presenting similar physicochemical characteristics than those obtained by long-thermal drying. Shrinkage also occurs during carbonization, this process involves a weight loss around 50 wt%, the main decomposition process takes place between 350–550 °C, being complete at around 800 °C.[61] Simultaneously, the gases release develops the microporosity of the system. Microporosity and surface area values however, tend to decrease with increasing carbonization temperature from 600 °C,[62] because very narrow micropores are formed. Nevertheless, the PSD can be fitted by physical[62] or chemical activation,[63] results being also dependent if the activation is carried out on the organic gels or on previous carbonized samples.

One of the main advantages of carbon gels regarding other CMs, besides the hierarchical porosity described, is purity, as they are synthesized from pure organic reagents. These pure carbon structures are active in different catalytic processes, including fine chemistry processes such as the synthesis of quinolines.[64] Nevertheless, carbon gels are mainly used as support of metallic active phases in the development of novel catalysts. The first option is the preparation of catalytically active metal-doped carbon gels by one-pot method, by solubilization of the corresponding metal precursors into the aqueous solutions of raw monomers, according to the procedure previously established.[65] Because these metals (namely transition metals) are catalytically active, they also influence on the different steps of the synthesis processes – polymerization, carbonization and activation – inducing changes in the porous texture[65–66] or graphitization degree.[66b] This procedure with several modifications is extensively used today for the preparation of metal-doped carbon gels.[67] Alternatively, metal-supported catalysts are obtained by classical methods – impregnation, CVD, etc. – using the previously optimized carbon supports and the appropriate active phases.[68] The stability, dispersion and performance of the active phases can be improved by previous functionalization of the carbon surface.[68–69] In addition, the morphology and nanostructure of carbon gels can be fitted by adding surfactants during the synthesis, allowing the preparation of highly-dispersed metallic nanoparticles on carbon gels structured as nanospheres, nanotubes, etc.[70] The metal dispersion, chemical and crystallographic characteristics of the active phases are strongly dependents of the interactions and links between supports and metallic precursors, leading to different active phases during the heat treatments.[66b,70–71] The sol gel procedure also facilitates the coatings of ceramic structures with a film of carbon gels, drastically modifying the hydrophilic character of typical cordierite honeycomb monoliths or foams and reinforcing their mechanical properties.[72]

Carbon-metal oxide – SiO_2, Al_2O_3, TiO_2, ZrO_2, etc – composites were also developed by co-polymerization of R–F solutions, as precursor of the carbon phase, with metal alkoxides, as metal oxide precursors.[73] The pre-gelation of the R–F carbon phase to define the nanostructure using surfactants, and the subsequent addition of the corresponding metal alkoxide, allows obtaining uniform metal-oxide coatings, forming nanostructured carbon core-shell materials that enhance the physicochemical properties and performance of the composite regarding the unsupported oxides.[74] There is a vast bibliography showing the potential application of this type of catalysts derived from carbon gels in many different fields, including electrochemistry,[69,75] Fischer-Tropsch reactions,[68] selective hydrogenations,[3d] environmental protection[74,76] and of course, fine chemical synthesis.[77]

2.3. Role of porosity and surface chemistry of carbons in catalysis

When designing/analyzing a catalyst, the discussion is always around how to achieve the pretended performance (conversion/selectivity) by controlling physical (particle size, morphology, porosity) and chemical characteristics (nature of the active site). The correct combination of these properties determines the best performance of materials, including the CMs under studying.

Basically, the relationship between porosity and catalytic performance is related with the balance between the pore size/molecular size/experimental conditions, in summary, with the diffusional restrictions to/from the active surface. However, the

reactivity of pure CMs is essentially associated with the presence of heteroatoms, unsaturated vacancies and defects located mainly at the edges of microcrystals, and delocalized π-electrons.[2c,78] OSGs are commonly induced on the carbon surface by oxidizing treatments in gas or liquid phase, leading to carboxylic acid, anhydride, phenol, carbonyl or ether groups. The surface enrichment by nitrogen or boron doping is also relatively easy, because both heteroatoms present a quite similar atomic size than carbon. *N*-functionalities act as electron-rich sites that attract electron deficient species and are actives in various organic transformations, including Knoevenagel condensation, aldol and Suzuki coupling reactions or the reduction of nitroarenes with hydrazine hydrate.[79] Phosphorous, Sulphur or Halogens are also incorporated mainly in the edges of the carbon structure using different approaches. These functionalities therefore determine the nature and strength of the interactions between the reactants and the surfaces, the adsorption modes, the formation of specific intermediates, the formation of deposits, among others.

In literature, there is a vast number of works focusing the importance of the localization of active sites in the adequate porosity range. The dehydration and dehydrogenation of alcohols have been traditionally used to determine the acid-basic character of surfaces.[80] Acidic groups favor the development of dehydration reactions leading to olefins and ethers, while dehydrogenation to aldehyde and ketones takes place preferentially on basic sites. This reaction (using ethanol) was carried out by Moreno-Castilla et al.[81] to characterize a series of ACs functionalized with OSGs. They prepared two ACs in steam, with increasing the activation degree from 20 (sample AZ20) to 46%, (AZ46), respectively. In this sense, the S_{BET} increased from 631 to 914 $m^2 g^{-1}$ and the mean micropore size (L_0) increased from 1.3 to 1.9 nm, as well the macro and mesoporosity. Both raw ACs present however a similar surface chemistry, with a pH of the point zero charge (pH_{PZC}) around 11. These samples were then oxidized with a saturated solution of $(NH_4)_2S_2O_8$ at 25 °C in periods of 0.5, 10 and 24 h. The oxygen content increased and the pH_{PZC} decreases as longer the treatment reaching $pH_{PZC} \approx 2$. The concentration of OSG fixed in AZ46 sample resulted around twice regarding AZ20. Catalytically, both raw ACs presented a low activity, independently of porous texture, and according to the basic character of their surfaces ($pH_{PZC} = 11$) both produced exclusively dehydrogenation (acetaldehyde). Conversions increased in both series with increasing the functionalization degree and the product distribution changed to produce dehydration, ethene and ether becoming the main products. No deactivation was detected in any case. However, they observed that functionalized ACs derived from AZ20 presented higher activity than those corresponding AZ46, in spite of the smaller porosity and functionalization degree of the former. This fact is discussed based on the localization of the active sites inside the porosity. The large size of the micropores developed in AZ46 allowed that acid groups were formed inside this porosity range, while in AZ20 catalysts were forced to be formed on the external surface. Under the experimental conditions used, reactions developed mainly on the acid groups placed on the external surface of the particles, thus, the large part of the active sites quantified for AZ46 resulted inactive.

Different types of CMs have been involved also in the synthesis or transformation of *N*-heterocycles. Perez-Mayoral et al.[82] compared different carbons (ACs from biomass, carbon xerogels and ordered carbons) in the synthesis of quinoxalines. The combination of a developed micro-mesoporosity and the OSG types in ACs influences on both activity and selectivity of the samples. These authors also prepared a series of carbon supported zirconia or sulfated zirconia involved on the selective green synthesis benzodiazepine, confirming that the presence of $-SO_3H$ functions on either zirconia or anchored onto the carbon surface, considerably improved the selectivity.[83] In addition, stronger acid sites anchored to the carbon surface and the high microporosity of ACs modified with different acids are responsible by the selectivity enhancement.[84] Much more recently, highly macroporous carbons from pyrolysis of spent tires to avoid diffusional restrictions, under mild reaction conditions, were also reported for benzodiazepine synthesis.[85]

The synthesis of heterocyclic compounds using CMs as recyclable catalysts was reviewed by Rai and Ranganath.[86] The influence of the characteristics and functionalization (metal complexes and metal oxides) of CNTs and CNFs and especially different types of *N*-functionalized porous CMs including graphitic carbon nitride (g-C_3N_4) on a wide collection of reactions were described. The work developed by van Deelen et al.,[87] as an example, shows the importance of surface characteristics on the distribution and catalytic behavior of active centers in this type of reactions. Because CNTs present convex and concave surfaces, the orientation of the substrate on the catalysts is crucial to obtain asymmetric catalysts. Anchoring the same chiral ligand, two opposite enantiomers of flavanone were synthesized.[87] Reversal enantioselectivity was also previously observed in the keto esters hydrogenation.[88]

Hydrogenation and dehydrogenation of *N*-heterocycles are important reactions for the synthesis of different types of valuable molecules. For example, unsaturated amines for the pharmaceutical industry are obtained by catalytic dehydrogenation of amines. Mesoporous g-C_3N_4 was used as support of bimetallic CoPd nanoparticles (NPs) to develop catalysts for the hydrogenation and dehydrogenation of quinolines and tetrahydroquinolines.[89] The use of mesoporous materials preserves the monodisperse particle size distribution avoiding the formation of aggregates. All tetrahydroquinoline substrates were successfully converted to the corresponding product with quantitative yields, using water as solvent and moderate temperatures, catalysts being stable and reusable. The mesoporous support not only stabilize the NPs distribution, but also is involved in electronic transfers with NPs. In the same context, ordered mesoporous carbons doped with *N*-functionalities (OMNCs) were used as Ru-supports for the hydrogenation of quinoline.[90] The high performance of catalysts is attributed to the interaction of *N*-dopants with Ru (strong electron donation to Ru) and the enhanced adsorption capacity on the pore structure of OMNCs. Results indicate a favorable interaction between quinoline and basic surface of mesoporous channels, improving diffusion and leading to a selective adsorption

towards pyridine ring, which accelerates the hydrogenation of pyridine rings preventing the hydrogenation of benzene rings.

On the other hand, GO presents a great concentration of OSGs and developed surface area. This material demonstrated a high performance in dehydrogenation reactions of *N*-heterocycles.[91] Using tetrahydroisoquinoline as the model substrate, blank experiments yield only 10% at 120 °C, which increased up to 92% using GO as catalyst. Other carbocatalysts, such as active carbon, acetylene black, and natural graphite, exhibited almost no catalytic activity in this reaction. Reaction took place on the OSGs and π-conjugated system of GO. Dehydrogenation reactions using metal-free catalyst (GO) are suitable to obtain valuable compounds such as quinoline, 3,4-dihydroisoquinoline, quinazoline, and indole derivatives.

Thus, different CMs with different morphology (1D, 2D, 3D), porosity and functionalization were used as catalysts or catalyst supports for the synthesis and transformations of *N*-heterocycles. The versatility of CMs is based on their capacity to fit these variables for specific applications.

3. Heterocyclic Synthesis Catalyzed by CMs

This section is organized considering the different types of heterocyclic compounds, only summarizing the synthetic strategies for building the heterocyclic core, through cascade reactions. Several examples of multicomponent reactions (MCRs), which allow the synthesis of structurally complex molecules in a safer, selective, efficient, faster, and economic manner, catalyzed by CMs as efficient and energetically favorable methodologies are also commented. It is important to note that MCRs are considered as greatly relevant synthetic methods used in both natural product synthesis and medicinal chemistry for drug discovery. Therefore, the development of green MCRs constitutes one of the challenges which pharmaceutical industry is facing.[92]

Subsequent sections describe the different synthetic approaches reported for each class of heterocycles with a different ring structure and that use carbon-based catalysts from the most traditional materials to more advanced ones. Sections classify the methodologies as a function of the type of heterocyclic system considering both ring size and number of nitrogen atoms.

3.1. Five-membered Rings

Five-membered heterocyclic rings containing nitrogen are substrates of capital importance mainly due to the broad spectrum of biological activities as anticipated. Next sections consider the different methodologies reported for the synthesis of five-membered *N*-heterocycles catalyzed by a great variety of CMs, starting from heterocycles containing one nitrogen atom to those with four ones.

3.1.1. Pyrrole and related compounds

Pyrrole derivatives are useful substrates for the pharmaceutical industry but also showing practical applicability in energy storage, and solar cells. This type of heterocycles is typically synthetized by Hantzsch and Paal-Knorr reactions, which often present many limitations in scope. Due to the diverse applications of pyrroles, a continuous search of cleaner methodologies is considered a relevant issue investigating modifications of this reaction or even reporting others more versatile synthetic strategies. In this context, Gong et al.[93] recently reported the one-pot synthesis *N*-substituted pyrroles *via* a Paal-Knorr condensation from nitro compounds with 2,5-hexadione catalyzed by a cobalt-nitrogen catalyst (Co-Nx/C-800-AT) at 110 °C during 10 h, in the presence of formic acid as hydrogen donor and co-catalyst, checking different solvents; the catalyst was prepared by the pyrolysis of cobalt phthalocyanine-silica colloid composites, and subsequent removal of silica template and cobalt nanoparticles (NPs).[94] It was observed important differences in conversion and selectivity ranging to null selectivity from dimethylformamide (DMF) to 90% when using EtOH. The reaction takes place through the sequence nitrobenzene reduction to aniline by transfer hydrogenation of formic acid over the Co-Nx/C-800-AT catalyst, and double condensation between aniline and 2,5-hexadione followed by double dehydration (Scheme 1).

Following another synthetic strategy, Pt^0-loaded carbon (Pt/C), prepared by the impregnation method on different commercially available carbons and pre-reduced in H_2 at 300 °C, have been reported as effective and reusable catalysts for the direct synthesis of 2,5-disubstituted pyrroles, through acceptor less dehydrogenative heterocyclization of 1,2-aminoalcohols and secondary alcohols, in diglyme at 125 °C, needing the presence of a base, particularly KO*t*Bu, among others explored (Scheme 2).[95] Pt/C catalysts yielded the corresponding 2,5-disubstituted pyrroles ranging from 86 to 92%, activity barely depending on the carbon support. As note, the catalytic performance of these carbon catalysts was superior to other Pt-loaded ones (*e.g.* on Al_2O_3, SiO_2, CeO_2, TiO_2, Nb_2O_5, ZrO_2, and H-BEA).

A more sophisticated strategy was reported for the one-pot synthesis of 2-phenyl indole by reacting 2-iodoaniline and phenylacetylene, in the presence of Et_3N, in a mixture of DMF/

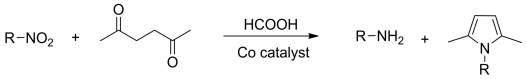

Scheme 1. Paal-Knorr condensation from nitro compounds with 2,5-hexadione catalyzed by Co–Nx/C-800-AT.

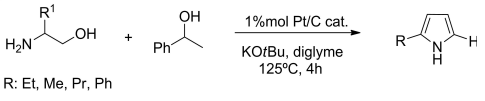

Scheme 2. Synthesis of 2,5-disubstituted pyrroles from 1,2-aminoalcohols and secondary alcohols catalyzed by Pt^0-loaded carbon catalyst.

H_2O (1:1), at 120 °C (Scheme 3), *via* domino reactions comprising Sonogashira C–C coupling reaction, hydrogenation, hydroamination, and heteroannulation, all of these steps catalyzed by commercially available Pd on AC catalysts (Pd/Cu/AC) and accelerated by the presence of CuI co-catalyst.[96]

Indolizines as other heterocyclic skeleton containing pyrrole ring have been successfully prepared by multicomponent synthesis of 2-pyridinecarbaldehyde derivatives, secondary amines and terminal alkynes, in CH_2Cl_2 at 70 °C, catalyzed by copper catalysts obtained by addition of the carbon supports (AC, graphite or MWCNT) to a suspension of CuNPs previously prepared from anhydrous copper(II) chloride, lithium metal, and a catalytic amount of 4,4′-ditert-butylbiphenyl in THF, at room temperature (Scheme 4).[97] CMs showed an enhanced catalytic performance regarding other Pd catalysts, in which Pd nanoparticles were supported on SiO_2, Ti_2O, Mont-K10, among others, yielding the corresponding indolizine from 73 to 92% of conversion (highest conversion value for Pd/C) *vs.* 21 to 68% when using other Pd-supported catalysts. Authors proposed that the formation of indolizines occurs *via* a copper-catalyzed aldehyde-amine-alkyne coupling, in which the corresponding propargyl amine is almost instantaneously formed. This intermediate undergoes the final cycloisomerization to give the desired product.

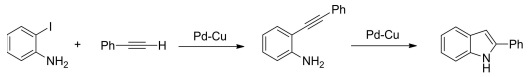

Scheme 3. Synthesis of 2-phenyl indole from 2-iodoaniline and phenylacetylene, in the presence of Et_3N catalyzed by Pd/C.

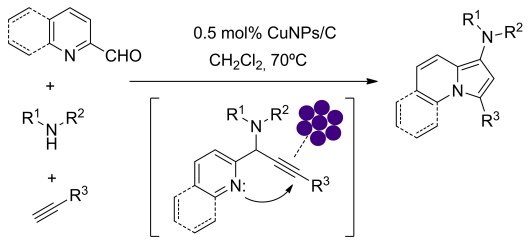

Scheme 4. Three-component synthesis of indolizines from 2-pyridinecarbaldehyde derivatives, secondary amines and terminal alkynes catalyzed by CuNPs/C.

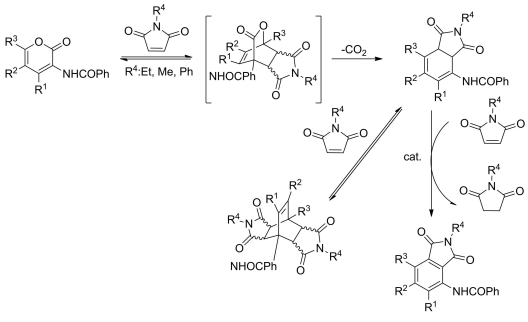

Scheme 5. Synthesis of isoindoles from 2*H*-pyran-2-ones and *N*-substituted maleimides catalyzed by DarcoKB.

An interesting example for the synthesis of isoindoles catalyzed by an AC (DarcoKB) from 2*H*-pyran-2-ones and *N*-substituted maleimides, in decalin as solvent, at 150 °C, was reported by Krivec et al. (Scheme 5).[98] The reaction firstly comprises a Diels-Alder cycloaddition between reagents followed by CO_2 elimination by retro-Diels-Alder reaction. Note that the last dehydrogenation step is key to selectively obtain the corresponding isoindole, since the resulting intermediate of the CO_2 extrusion can undergo a second cycloaddition with *N*-substituted maleimides yielding a by-product as double-cycloadduct. Authors explored several CMs as dehydrogenation catalysts including DarcoKB AC, MWCNTs and SWCNTs as well as CMs containing precious metals such as Rh/C, and Pd/C, correlating the S_{BET} surface area with the dehydrogenation capability; DarcoKB AC was found to be the most efficient catalyst leading to the corresponding isoindole with quantitative conversion and total selectivity. Additionally, it was observed that the final aromatization step takes place by hydrogen transfer to maleimide affording succinimide promoted by the active surface of the CM catalyst.

3.1.2. Pyrazole and related compounds

Pyrazoles are commonly synthetized by cyclocondenzation of 1,3-diketones and hydrazines in the presence of great variety of acid catalysts. Concerning to that, Fe/MWCNT catalysts containing zero-valent iron nanoparticles was reported for the facile synthesis of pyrazoles obtained in good-to-excellent yields, in EtOH, at room temperature (Scheme 6).[99] MWCNTs were prepared by CVD at 1300 °C, by using acetylene and ferrocene, as carbon and iron nanoparticles sources, respectively. As note, traces of oxygen during the MWNCT formation resulted in the formation of carboxylic acid functions at the surface. In the case of using asymmetric 1,3-dicarbonyl compounds such as ethyl acetoacetate, the corresponding oxo-pyrazole as mixture of both enolic and keto forms was obtained. It is noteworthy that Fe/MWCNTs can be considered as a highly versatile catalyst useful for the synthesis of a great variety of *N*-containing heterocycles, through MCRs including highly substituted piperidine even bis-spirosubstituted piperidines, dihydro-2-oxoyrroles, among others, under mild reaction conditions.

Zakeri et al.[100] developed water dispersible phosphonated graphene oxide catalysts (GO-PO_3H_2) by following the sequential protocol comprising i) graphite oxidation, ii) exfoliation and iii) subsequent phosphonation. This last step consisted of the

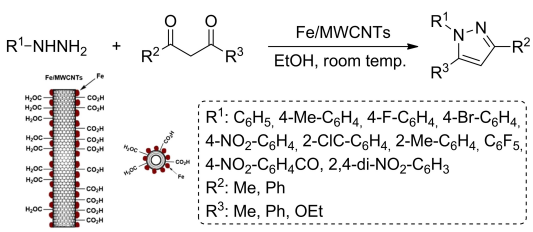

Scheme 6. Synthesis of pyrazole derivatives catalyzed by Fe/MWCNTs.

treatment of GO with a mixture of polyphosphoric acid and phosphoric acid upon sonication, at pH of 5, and after that heated at 95 °C during 5, 10 or 15 h. Combined results of Fourier-transform infrared spectroscopy (FTIR) and x-ray photoelectron spectroscopy (XPS) demonstrated the presence of P–O, C_{ring}–P and P=O and C–P and P–O–C functionalities after phosphonation, besides OSGs from the oxidized carbon surface. O/C ratio ranging from 0.498 in GO to 0.44 in GO-acid-III, the most phosphorylated sample, whereas P/C ratio was increased from 0 to 0.125. In this case, the catalysts under study were explored in MCRs for the synthesis of more complex heterocycles containing the pyrazole ring, pyrano[2,3-*c*]pyrazoles, from hydrazine hydrate, ethyl acetoacetate, benzaldehyde and malononitrile in water at reflux, the presence of GO-acid-II(10 h) selectively yielding the desired product in 90% after 15 min of reaction time (Scheme 7). This methodology widely tolerates differently functionalized benzaldehydes in scope, the catalyst being reusable at least during 6 cycles without activity loss.

A tentative reaction mechanism comprising the simultaneous formation of both intermediate species, arylidenemalononitrile **A**, resulting of Knoevenagel condensation between benzaldehydes and malonitrile, and pyrazolone **B** by ciclocondensation of ethyl acetoacetate and the corresponding hydrazine, was proposed. Subsequent Michael addition between both intermediates followed by heterocyclization reaction would afford the corresponding complex pyrazole. Authors highlighted that the amphoteric character of the GO–PO_3H_2 is behind the observed reactivity.

Synthesis of fully functionalized pyrazoles obtained in high yields (up to 82%) from benzaldehydes, malononitrile and phenylhydrazine in the presence of GO–TiO_2 composites, in water, at room temperature, have been also reported (Scheme 8).[101] GO–TiO_2 was prepared from GO and Ti(O*i*Pr)$_4$ in isopropyl alcohol. In this case, GO–TiO_2 showed functionalities of GO but also Ti–O–Ti, and C–O–Ti interactions demonstrating that TiO_2 nanoparticles are immobilized on GO.

3.1.3. Imidazole and related compounds

Imidazoles and benzimidazoles are *N*-containing heterocycles exhibiting a broad spectrum of biological activities but also contained in relevant life molecules, such as histamine and histidine. These compounds, mainly imidazole derivatives, are extensively used in the synthesis of ionic liquids (ILs) with a great potential as green solvents and even as catalysts, as anticipated.

Synthesis of 2,4,5-trisubstituted imidazoles generally consists of multicomponent cyclocondensation of 1,2-diketone, α-hydroxyketone or derivatives with aldehydes and ammonium acetate in the presence of a great variety of acid catalysts. However, this methodology often requires prolonged reaction times to obtain worse yields and difficult work-up procedures, originating contaminant waste together high costs, among some disadvantages.

CMs are also investigated for this transformation implying different approaches for both the catalyst preparation and the synthesis of the imidazole derivatives. Hanoon et al.[102] developed an acid catalyst consisting of fluorinated GO (A-MFGO) (Scheme 9) for the synthesis of 2,4,5-triarylimidazole derivatives (81–95% of yield) from benzyl, different aldehydes, and ammonium acetate, in ethanol at reflux, showing a superior catalytic performance than other traditional catalysts (*e.g.* H_2SO_4, [IL](bmim)SO_3H or $H_3[P(W_3O_{10})_4]$). In a similar way, a GO-chitosan bionanocomposite has been also reported for an one-pot three-component synthesis of trisubstituted imidazoles (yield up to 80%), in absence of any solvent at 120 °C, from benzyl or benzoin and substituted benzaldehydes[103]

Water-soluble phosphorylated GO catalysts synthetized through different chemical and thermal conditions were also reported for benzimidazole synthesis.[104] Firstly, GO was functionalized with phosphate moieties (PGO) in the presence of phosphorus trichloride and triethylamine, in tetrahydrofuran (THF), and subsequently thermally treated at 250 or 400 °C and hydrolysis; PGO-400 showing high surface area, water dispersibility and special electrical conductivity. The catalysts were assayed in a facile and green two-component synthesis of benzimidazole from *o*-phenylenediamine and substituted benzaldehydes, in EtOH, at room temperature, selectively affording the desired product in excellent yields (87-94% after 45–90 min) (Scheme 10).

Interestingly, Weires et al.[105] reported the selective one-pot synthesis of a plethora of 2-aryl-benzimidazoles from *o*-nitroanilines and different substituted aldehydes by combining both Pd/C and montmorillonite-K10 compatible catalysts through the sequence transfer hydrogenation-condensation-dehydrogenation reactions (Scheme 11). While Pd/C catalyst is responsible of the transfer hydrogenation and dehydrogenation reactions, Mont-K10 acts as an acid catalyst for condensation between the formed diamine and aldehydes. Note that the initial reduction of the nitro group in *o*-nitroanilines is catalyzed by Pd/C in the presence of NH_4HCO_2, as hydrogen donor, at toluene reflux, while Mont-K10 promoted the subsequent condensation with the corresponding aldehyde at lower temperature. The cooling in this step, before adding the corresponding aldehyde to the reaction mixture, is key for the selective synthesis of 2-subtituted benzimidazole observing the formation of 1,2-disubstituted benzimidazole only at trace levels.

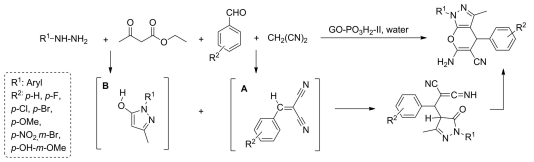

Scheme 7. Synthesis of pyrano[2,3-*c*]pyrazoles catalyzed by GO-PO_3H_2.

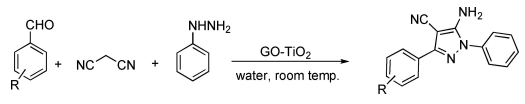

Scheme 8. Synthesis of pyrazoles from aldehydes, malononitrile and thiophenol, in water, at room temperature, catalyzed by GO-Ti_2O.

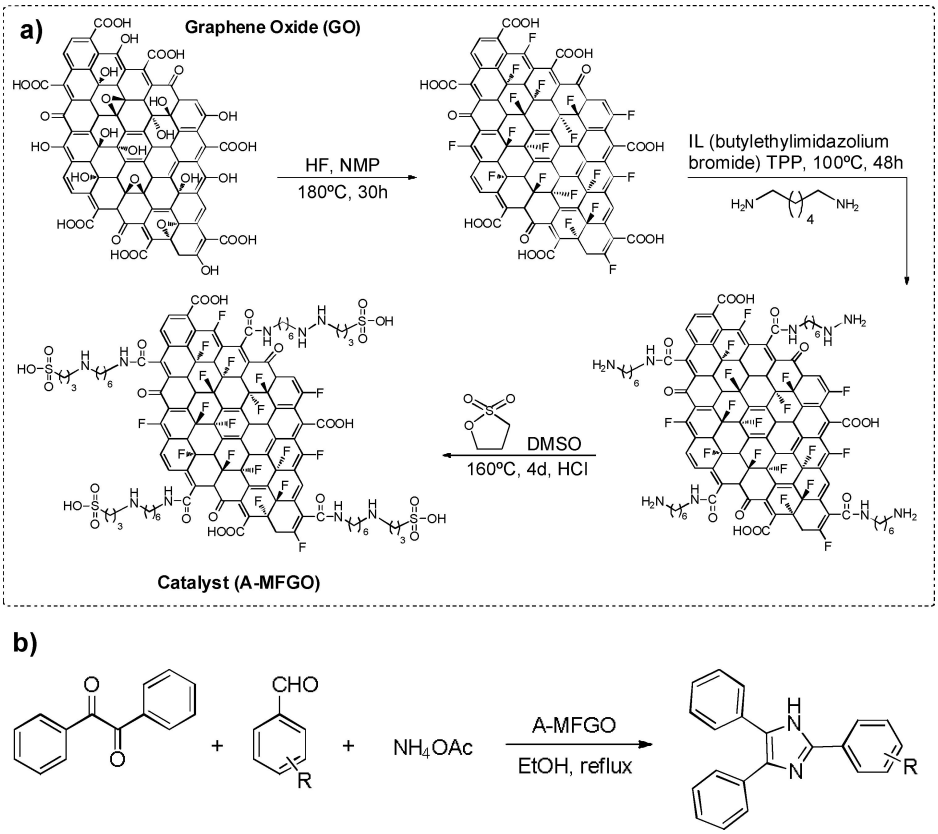

Scheme 9. a) GO-derived catalyst prepared by the sequence i) fluorination, ii) amidation, iii) reaction with γ-sultone. b) Synthesis of 2,4,5-triarylimidazole derivatives from benzyl, substituted benzaldehydes and ammonium acetate catalyzed by A-MFG.

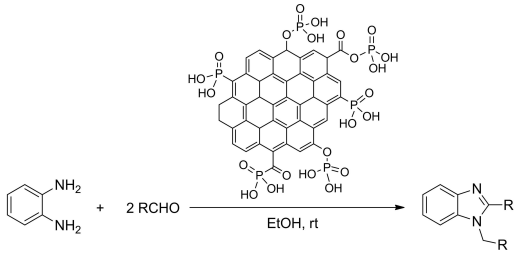

Scheme 10. Synthesis of 1,2-substituted benzimidazoles catalyzed by PGO.

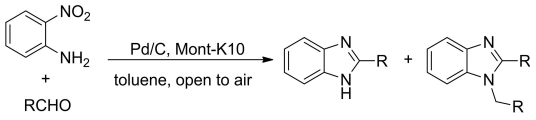

Scheme 11. Selective synthesis of 2-arylbenzimidazoles in the presence of both Pd/C and Mont-K10 catalysts.

Much more recently, Lin et al.[106] implemented a similar strategy by using a robust catalyst consisting of Co^0 nanoparticles encapsulated in *N*-doped CNTs (Co@N-CNT900) exhibiting a mesoporous character and high S_{BET} (648 m^2/g), in which Co-N_x interactions were demonstrated; the sample was synthesized by pyrolysis of a mixture containing pluronic P123, melamine and cobalt acetate, at 900 °C, the pyrolysis temperature directly impacting on the architecture of Co@N-CNT samples. This catalyst was tested in the reaction of 2-nitroaniline and benzaldehyde in ethyl acetate, at room temperature, under H_2 atmosphere yielding 2-phenyl-benzimidazole in quantitative conversion and total selectivity, also tolerating the substitution on the aromatic ring of nitroaniline. Note that in this case when using CMs, the reaction requires mild reaction conditions compared to the combined mixture of catalysts above referred. This catalyst was also assayed in the reaction between 1,2-dinitrobenzene with differently substituted benzaldehydes and other heteroaryl aldehydes affording the desired products in 64–98% of yields. Authors also reported a theoretical study, based on DFT calculations, concerning the hydrogenation of nitroaniline step by step, calculating the activation and dissociation of H_2 on the surface of the two catalyst models, comprising the Co catalyst (Co_4@N-CNT) and the corresponding metal-free N-CNT, concluding that the hydrogenation reaction in the presence of Co_4@N-CNT occurs with lower energy barrier.

A more sophisticated strategy to prepare a recyclable and efficient catalyst for dehydrogenative coupling of benzyl alcohol and *o*-phenylenediamine was reported by Shaikh et al.[107] (Scheme 12). The catalyst consisted of magnetic nanofibers (MNF), prepared from magnetite nanoparticles reacting with different ligands such as benzene-1,4-dicarboxylic acid, 1,3,5-benzene-tri-carboxylic acid or 1,2,4,5-benzene-tetracarboxylic acid, and confined into CNTs, both interacting by strong π,π-

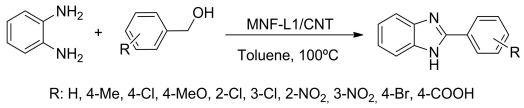

Scheme 12. Synthesis of 2-aryl-benzimidazole derivatives catalyzed by MNF-1/CNT.

stacking and therefore, favoring a high nanoparticle dispersion. In this way, it also prevents the nanoparticle aggregation increasing the stability and recyclability of the catalyst. MNF-1/CNT (where 1 stands for as benzene-1,4-dicarboxylic acid) resulted the most efficient catalyst selectively affording the corresponding benzimidazole in 92%, after 2 h of reaction time, in toluene at 100 °C. This reactivity was attributed to the proper orientation of the bulk ligand inside the CNT channels.

3.1.4. Triazoles

Click chemistry is an undoubtedly powerful technique consisting of a set of reactions to produce the desired product in high yields, in a stereospecific manner, preferentially no generating by-products and resulting in a broad scope, according with the definition provided by K. B. Sharpless. Its application has been demonstrated in multiple researching fields and particularly for the fast synthesis of relevant biologically heterocyclic scaffolds. One example of it, is the alkyne-azide cycloaddition reaction affording 1,2,3-triazole as an interesting pharmacophore.[108] In addition, 1,2,3-triazoles are considered versatile bio-isosteres of numerous functional groups such as amide, ester, carboxylic acid, olefins, vastly used in drug discovery.

The alkyne-azide cycloaddition reaction is significantly accelerated by Cu^{I} species, although $CuSO_4$ in the presence of sodium ascorbate is the preferred option in aqueous medium, to *in situ* generate the active Cu^{I}. Then, CMs emerge as an opportunity to produce Cu^{I} supported catalysts, the carbon matrix acting as reducer. In this context, Lipshutz and Taft[109] reported a cheap, easily prepared and robust material composed by copper-in-charcoal (Cu/C) obtained by impregnation of activated wood charcoal (Aldrich, 100 mesh) with $Cu(NO_3)_2$ in water, under ultrasound irradiation, in which both CuO and Cu_2O were dispersed over the carbon matrix. The Cu/C catalyst resulted highly efficient in alkyne-azide cycloaddition at 60 °C in dioxane, giving the corresponding triazole in excellent yields. Authors highlighted the impact of using triethylamine, notably decreasing the reaction time from 4 h to 4 min when reacting benzyl azide and 1-methyl-3-butyn-2-ol (Scheme 13a). Solvents such as toluene, ethanol or even, water were also analyzed leading to the corresponding triazole with yields up to 97%. In addition, triazole-containing steroidal derivative was also prepared in good yield (35–99%).

A similar study was reported by Lee et al.[110] using the Cu/C catalyst for tandem diazo transfer/click reactions. While small amounts of CuO in the Cu/C catalyst are able to catalyze the diazo transfer reaction from TfN_3 to amines, Cu_2O promotes the cycloaddition of the formed azide to the corresponding alkyne,

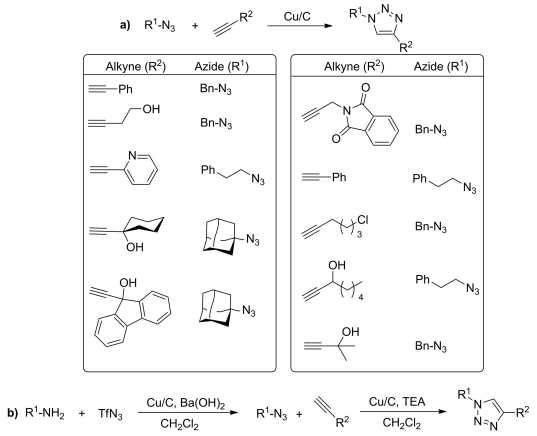

Scheme 13. a) Synthesis of substituted 1,2,3-triazoles from organic azides and terminal alkynes; b) tandem azide formation/click reaction.

this last under conventional heating (40 °C in CH_2Cl_2) or even as microwave-assisted reaction, in this case considerably reducing the reaction time (Scheme 13b).

A more sustainable multicomponent synthesis of substituted triazoles from different precursors including azide, organic halides, diazonium salts, anilines and even epoxides, in water at 70 °C, in absence of any base, catalyzed by copper nanoparticles on ACs with low copper loading (1.6 wt%) has been also reported (Scheme 14).[111] Different carbon supports were analyzed such as graphite, MWCNTs and ACs beside other structurally different materials including SiO_2 and Al_2O_3, in all the cases affording yields up to 90% after 9 h.

Highly dispersed copper nanoparticles have been also immobilized onto graphene nanosheets and applied to the synthesis of triazoles. Nia et al.[112] and Li et al.[113] used GO to synthesize the catalysts. Both methodologies include the use of GO treated with the corresponding copper salt, acetate or sulfate. In the first approach Cu(II)/GO was submitted to thermal treatment (600 °C) and reduced under Ar atmosphere to give TRGO/Cu, whereas Cu–Cu_2O@RGO composite (21.65 wt% of Cu content) was obtained following a one-pot synthetic procedure by adjusting the pH to 9, and subsequent addition of polyvinylpyrrolidone (PVP) and glucose and heated at reflux.

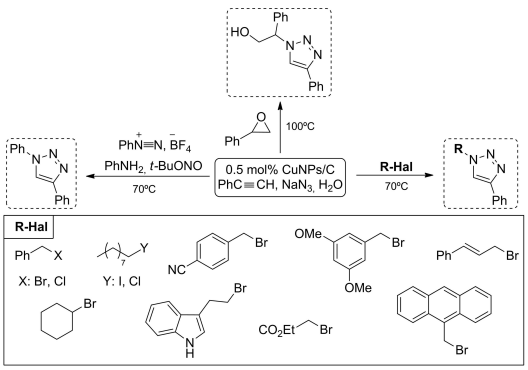

Scheme 14. Synthesis of 1,2,3-triazoles from phenylacetylene with different azide precursors catalyzed by CuNPs/C in water.

Both catalysts resulted in high activity for azide/alkyne click chemistry between benzyl azide and phenyl acetylene or tandem reaction of halides and sodium azide with terminal alkynes, using mixtures of water/alcohols (methanol or ethanol), at room temperature, selectively affording the corresponding triazole in high yields (up to 93%).

Different Cu^{I}-complexes anchored to GO applied to the synthesis of triazoles, under sonication, and using different precursors have been also studied.[114] Such is the case of a supported Cu^{I}-complex derived from polytriazoles on GO-(GO@PTA–Cu) (Scheme 15) twistedly prepared by using the referred azide/alkyne click chemistry but also applied to the synthesis of triazoles from styrene oxide, phenylacetylene and NaN_3 under sonication in water (Scheme 14).[114]

Although the Cu^{I} catalysts are the most popular ones for this transformation, other alternatives have also been reported. For instance, Salam et al.[115] investigated a silver-graphene nanocomposite (Ag–G) (Scheme 16) actives in the one-pot two step click reaction from aromatic azides, originated from the corresponding anilines, and alkynes under mild reaction conditions (water, room temperature) reaching the corresponding triazoles in high yields (up to 89% after 8–10 h).

Rossy at al.[116] reported an interesting approach to synthesize 1,2,3-triazoles comprising of one-pot sequential Sonogashira-Click reactions promoted by Pd–Cu/C multi-task catalyst

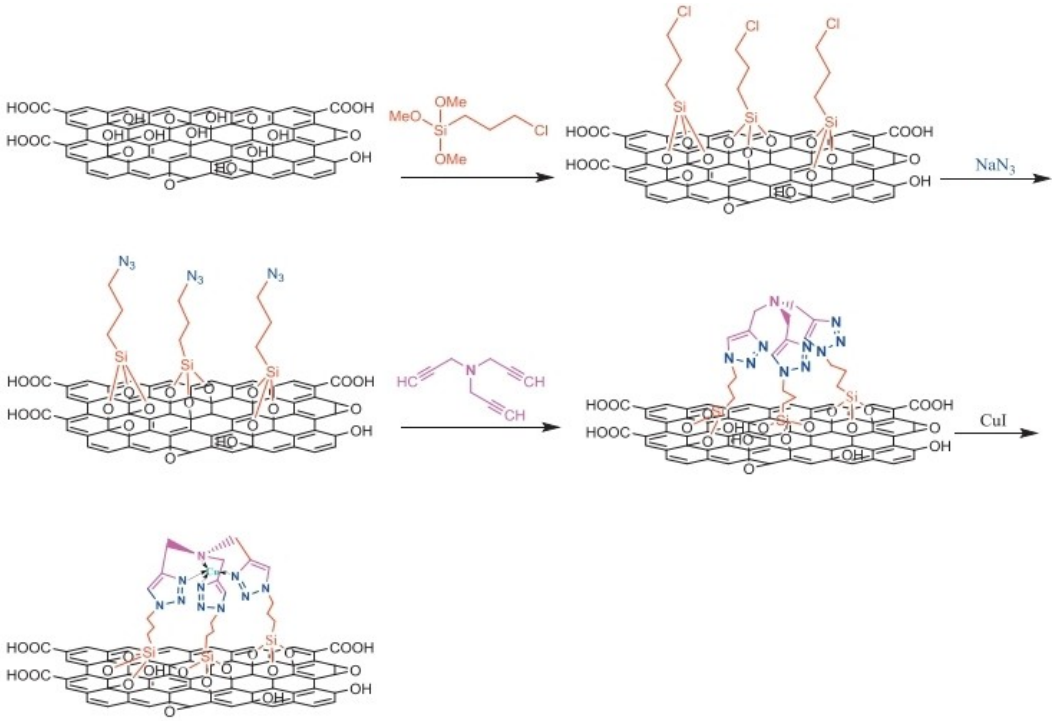

Scheme 15. Preparation of GO@PTA–Cu organocatalyst. Reproduced from ref. [114] Copyright (2017), with permission from Elsevier.

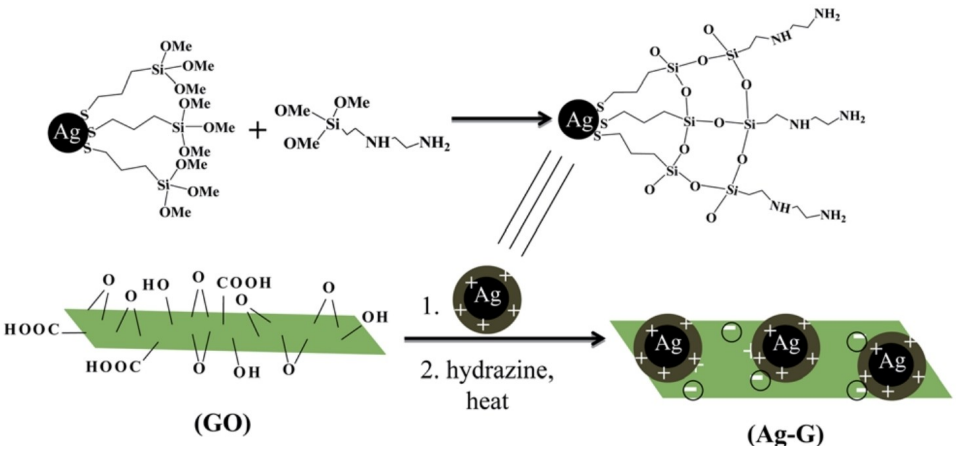

Scheme 16. Synthetic method for silver-graphene nanocomposite (Ag–G). Reproduced from ref. [115] Copyright (2014), with permission from Royal Society of Chemistry.

(Scheme 17). The catalysts were easily prepared from a solution of $Pd(OAc)_2$, $Cu(OAc)_2$ and activated charcoal, in MeOH stirred under H_2 atmosphere. In Pd–Cu/C catalysts, monometallic particles coexist with the bimetallic ones observing zones enriched with copper and/or palladium. Pd was found as both Pd^0 and Pd^{2+}, suggesting the formation of Pd–O bonds at the nanoparticle surface by fast aerobic oxidation of Pd^0 nanoparticles, whereas Cu is as $Cu^0/Cu^+/Cu^{2+}$. This methodology was also compatible with benzyl or aliphatic azides.

Much more recently, MOF-derived Cu@N–C catalysts were reported for the investigated transformation. By one side, Yamane et al.[117] employed Cu(BTC), where BTC is benzenetricarboxylic acid, under high-pressure and high-temperature treatments, yielding a copper-carbon composites (Cu@C), containing fine Cu^0 together Cu_2O and CuO nanoparticles; the Cu content increasing with the temperature (Cu = 63 wt% at 5 GPa/500 °C), and showing a low S_{BET} (0.4–22.6 m^2/g). Cu@C composites exhibited a high activity in the synthesis of the corresponding triazole from benzyl azide and phenylacetylene, in the presence of triethylamine and dioxane as solvent, at 60 °C, increasing it with the pyrolysis temperature. Interestingly, Wang et al.[118] developed a series of Cu-supported on *N*-doped porous carbons (Cu@N–C) from copper(II) bisimidazolate ($Cu(im)_2$) submitted to pyrolysis at different temperatures (400, 600, 800 °C), under Ar atmosphere, able to catalyze the one-pot multicomponent synthesis of 1,4-disubstituted 1,2,3-triazoles through 1,3-dipolar cycloaddition of aryl halides, sodium azide and terminal alkynes. Although the referred composites showed a homogeneous distribution of nitrogen, Cu nanoparticles gradually formed aggregates when increasing the pyrolysis temperature, Cu^{2+} being reduced to Cu^0 at the highest temperature and also increasing the Cu^0 content. Among the investigated samples, Cu@N–C(600) resulted in a high activity, even superior to the traditional catalytic system ($CuSO_4$/sodium ascorbate), for the cycloaddition reaction between benzyl bromide, sodium azide, and phenylacetylene leading to the corresponding 1,2,3-triazole in high yield (94%), in water at 50 °C, in absence of any base. The reported methodology tolerates a great variety of functional groups being investigated in a broad substrate scope.

3.1.5. Tetrazole

Tetrazole derivatives present a great diversity of applications. Besides the pharmacological activities, these compounds are useful in photo-imaging, as chelating agents, lubricants but also as herbicides and fungicides. Among the different catalysts reported for tetrazole syntheses, CMs such as graphene[119] or GO/ZnO nanocomposites[120] presented either a very low reusability or moderated yields or both. On the other hand, Yildiz et al.[121] reported a new methodology to prepare tetrazole derivatives in high yields (up to 90% after 8–20 min), from benzonitriles and NaN_3, catalyzed by Pd/Co nanoparticles decorated MWCNTs (PdCo@CNT) under microwave irradiation, at lower temperature (80 °C *vs* 120 °C), in DMF (Scheme 18). PdCo@CNT presented a high S_{BET} and monodispersed Pd^0 and Co^0 nanoparticles resulting highly active, stable and showing a great durability.

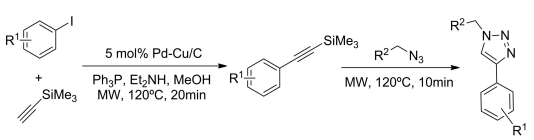

Scheme 17. One-pot sequential synthesis of triazoles through Sonogashira-Click reactions approach.

3.2. Six-membered Rings

3.2.1. Pyridines, quinolines and related compounds

Among the representative pharmaceuticals containing the pyridine or quinoline rings are loratadine, lansoprazole, pioglitazone used for allergies treatment, ulcers, and diabetes, respectively, whereas quinine, papaverine, emetine are examples of biologically natural-occurring products as alkaloids. Different green approaches and catalysts have been applied to the synthesis of this abundant heterocyclic core. Such is the case of recently reported, reusable and magnetically separable Fe_3O_4-decorated MWCNTs highly active in the preparation of polysubstituted pyridines (yield up to 80%), in water at reflux, from 1-aryl propan-2-ona, cinnamaldehyde and ammonium acetate (Scheme 19).[122] MWCNTs were prepared by CVD, using iron oxide nanoparticles as catalytic template, which were treated with Fe_3O_4 nanoparticles, under sonication, previously formed from $FeCl_2 \cdot 4H_2O$ and $FeCl_3$, in water, in the presence of *Astragalus membranaceus* extract, a perennial plant from China and Korea whose roots are used with medicinal purposes. In this case, Fe_3O_4 nanoparticles were covering the outer MWCNT surface.

Highly functionalized pyridines (yield up to 81%) have been also reported by multicomponent synthesis from aldehydes, malononitrile and thiophenol, in water, at room temperature, in the presence of GO-TiO_2, this catalyst being before related with the synthesis of pyrazole derivatives (Scheme 20).[101]

Interesting and highly useful biologically related compounds contain 1,4-dihydropyridine (1,4-DHP) skeleton, com-

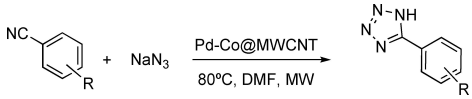

Scheme 18. Synthesis of tetrazoles from benzonitriles and NaN_3 catalyzed by PdCo@CNT.

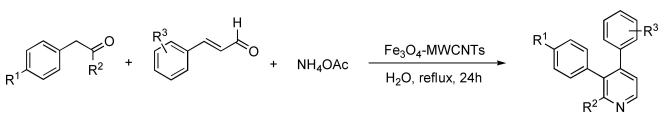

Scheme 19. Synthesis of polysubstituted pyridines from 1-aryl propan-2-ona, cinnamaldehyde and ammonium acetate, in water at reflux, catalyzed by Fe_3O_4- MWCNTs.

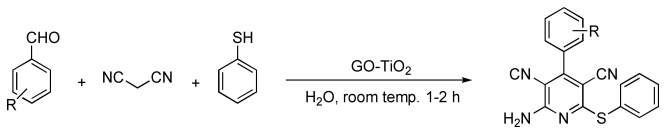

Scheme 20. Synthesis of pyridines from aldehydes, malononitrile and thiophenol, in water, at room temperature, catalyzed by GO-Ti_2O.

monly prepared by Hantzsch synthesis, consisting of MCR between an aldehyde, α,β-keto ester and ammonium acetate as nitrogen source. Different structurally catalysts have been reported for the Hantzsch synthesis although often requiring hard reaction conditions and long reaction times beside complex and tedious work up protocols.

In this context, following a modified synthetic approach, Co_3O_4-CNTs have been also reported for the four-component synthesis of asymmetric 1,4-DHP, in EtOH, at 50 °C, under ultrasound irradiation, in a facile and rapid approach (97% in only 15 min) as compared to conventional heating conditions (95% after 40 min) (Scheme 21).[123] The catalyst was prepared from oxidized MWCNTs by treatment with $Co(NO_3)_2 \cdot 6H_2O$ dissolved in *n*-hexanol and refluxed at 140 °C, in such a manner that the presence of OSGs favours the high dispersion of Co_3O_4 nanoparticles at the external walls.

GO catalyst have been also used for the synthesis of 1,8-dioxoacridines by replacing ammonium acetate by anilines. Aday et al.[124] reported GO as highly efficient catalyst for the synthesis of the corresponding acridines (Scheme 22), in DMF at 100 °C, obtaining higher yields (95% after 90 min) than other traditional acid catalysts such as Amberlyst-15 (72% after 5 h) or *p*-toluensulfonic acid (78% after 5 h).

Another type of nitrogen-containing heterocycles widely distributed in nature and synthetic drugs are quinolines. Several CMs showing different morphology, porosity and composition have been reported for the synthesis of this class of heterocycle. López-Sanz et al.[125] reported a new series of acid ACs, from commercially available carbons – Norit RX3 and Merck – submitted to acid treatment with HNO_3(N) and H_2SO_4(S), catalyzing the reaction between 2-aminoaryl ketones and ethyl acetoacetate, at 90 °C, *via* Friedländer condensation (Scheme 23), as the most cited and useful reaction to obtain quinolines, in high conversion (up to 93%) and moderate selectivity.[126] Authors proposed that the combination of both texture and the acid character of the catalysts influenced on the reaction selectivity. The Norit/S catalyst, a microporous sample with high S_{BET} (1114 m^2/g), and –SO_3H functions at the carbon surface, promoted the Friedländer condensation in high conversion (98% after 4 h) leading to mixtures of quinoline/quinolone in 75:23 ratio. In addition, the theoretical calculations suggested that the high selectivity of these CMs containing sulfonic acid groups could be due to the low flexibility in the reaction intermediates. Following a similar strategy, different acid carbon aerogels, prepared by R–F polymerization, have been also investigated in the Friedländer reaction[64] between 2-amino-5-chlorobenzaldehyde and ethyl acetylacetate, under solvent-free conditions, at 50 °C, upon conventional heating or microwave irradiation. Combining both experimental and theoretical results, based on DFT calculations, the authors proposed that the reaction follows the sequence: i) aldolization, ii) heterocyclization and iii) aromatization by double dehydration, where OSGs, in particular –CO_2H, are involved in each reaction step acting as individual catalytic sites. In addition, relatively strong π–π-stacking interactions between carbon support and reagents could contribute to the observed reactivity promoting the first aldolization step.

Based on this study, a new set of transition metal-doped (Ni, Co or Cu) carbon aerogels, prepared by introducing the corresponding metal precursor in the R–F mixture, active in the Friedländer reaction, has been developed.[127] In this case, the most active catalyst was the RFCoS sample, in which the Co^0 nanoparticles are the predominant active catalytic specie, yielding the corresponding quinoline in 93% after 60 min. Enhanced yields to quinoline in the presence of Co^0-doped aerogel are probably due to the high nanoparticle dispersion over carbon surface. A similar study comprises the development zero-valent cobalt-doped but also supported on carbon aerogels efficiently catalyzing the reaction of 2-amino-5-chlorobenzaldehyde and β-ketoesters at 50 °C, under solvent-free conditions.[128] This study allowed to correlate both the catalyst structure and the catalytic performance also analyzing other parameters such as the carbonization temperature and surface chemistry modification. The most efficient Co-doped aerogel was that prepared at low carbonization temperature (500 °C) showing a high metal nanoparticle dispersion and well-developed mesoporosity, selectively yielding the corresponding

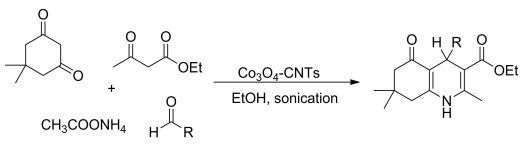

Scheme 21. Synthesis of polyhydroquinolines dimedone, aryl aldehydes, ethyl acetoacetate and ammonium acetate in the presence of Co_3O_4-CNTs.

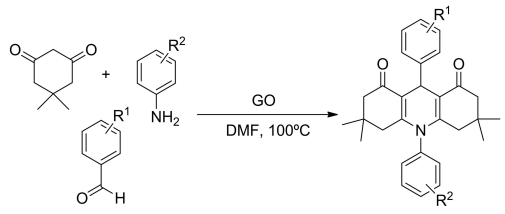

Scheme 22. Synthesis of acridines from aldehydes, anilines and dimedone, in in DMF, at 100 °C, catalysed by GO.

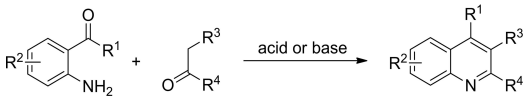

Scheme 23. Friedländer condensation between 2-aminoarylaldehyde/ketones and carbonyl compounds with active methylene groups. Reproduced from ref. [125] Copyright (2009), with permission from American Chemical Society.

quinoline in high conversion (93% after 30 min). The main disadvantage of this catalyst was probably related with the presence of some inactive metal particles, which were surrounded into the porous matrix, and not accessible to reactants. In contrast, Co-supported catalyst (B500-3%Co) showing a lower metal loading (3% *vs* 5.8%) was the preferred one because metallic nanoparticles were located at the carbon surface and in direct contact with reactants, yielding the corresponding quinoline in quantitative conversion in only 15 min. In addition, the effect of the surface chemistry when using the corresponding aerogels submitted to oxidant treatment with H_2O_2 was analyzed, the presence of OSGs leading to worse catalytic performances. Considering that, a novel series of eco-sustainable catalysts based on CoO nanoparticles supported on different carbon supports and applied to the synthesis of quinolines, under the same reaction conditions, have been also reported.[77a] In this case, different metal loadings (1, 3 and 5%) were supported on i) commercial Norit carbon, ii) oxidized commercial CNTs (CNT_{ox}) and, iii) a carbon aerogel calcined at 500 °C (B500). All of them were efficient and selective in the synthesis of quinolines, conversions up to 80% being obtained in the presence of CNT_{ox}3Co, B5003Co or Norit3Co, after 2 h, under mild reaction conditions (30 °C). In this way, this study allowed to conclude that all aspects influencing accessibility, including porosity, concentration and metal phase dispersion, strongly affect to the catalyst activity.

In other context, Godino et al.[129] reported a new series of carbon basic catalysts (PET/MAG) supporting MgO crystals of different size that efficiently and selectively promote the Friedländer condensation between 2-amino-5-chlorobenzaldehyde and ethyl acetylacetate, under free-solvent conditions, and at room temperature. Catalysts were prepared by the pyrolysis of homogeneous mixtures of poly(ethylene terephthalate) (PET) and magnesite (MAG), as carbon and MgO precursors, at 650 °C; in this case, the conversion to quinoline increased as function of MgO loading. In addition, the reaction mechanism for the synthesis of quinolines was theoretically investigated, by using computational calculations, considering that MgO is the predominant active catalytic specie. This study strongly suggested that the reaction occurs by i) dissociative chemisorption of ethyl acetoacetate, through the carboxylic oxygen of the –CO_2Et group, ii) C–C bond formation, iii) heterocyclization, assisted by two water molecules, iv) dehydratation and, v) aromatization, leading to the corresponding quinoline (Scheme 24). In a similar context, Godino-Ojer et al.[77b] developed highly efficient and sustainable ZnO-supported CMs for the synthesis of quinolines under the reaction conditions commented above (at 30 °C). The catalysts were prepared from the previous mentioned carbon supports – CNT_{ox}, Norit RX3 and B500 – by impregnation with aqueous solutions of Zn-$(NO_3)_2 \cdot 6H_2O$, followed by thermal treatment. It allowed to conclude that catalytic activity was affected by the nature of the support, the samples with lower Zn loading showing a conversion that increased following the order B5001Zn < CNT_{ox}1Zn < Norit1Zn, suggesting a negative effect of the mesopores on the catalytic performance of the series. Moreover, the conversion increased with ZnO loading, the Norit3Zn catalyst being the most effective in quinoline synthesis (96% after 15 min). Therefore, the combination of Zn loading with the developed porosity of the selected carbon support seems to be the key factors determining the catalytic performance.

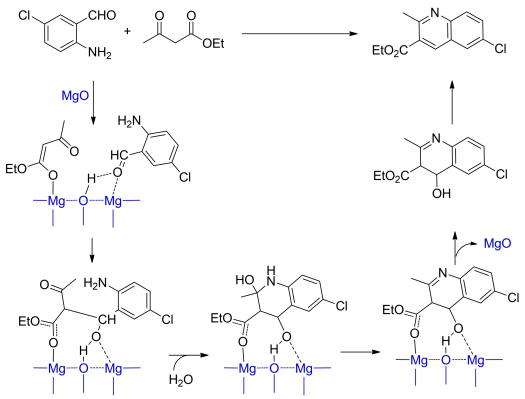

Scheme 24. Reaction mechanism for the Friedländer reaction between 2-amino-5-chlorobenzaldehyde and ethyl acetoacetate catalyzed by MgO-supported CMs.

Interestingly and as unique example, Chen at al.[130] reported carbon-based SACs – Fe, Co, Ni, Cu – highly efficient and selective (68% approximately) in the oxidative cyclization of anilines and acetophenones in the presence of DMSO, at 120 °C, under O_2 atmosphere. The superior performance was attributed to the hierarchical porosity of the material, the accessibility of the active centers probably comprising metal-N_4 coordination sites, but also the relatively weak desorption energy of the product.

3.2.2. Quinoxalines

Quinoxalines are often synthetized from diamines and 1,2-dicarbonyl compounds or precursors, a huge number of structurally different catalysts being reported. In this context, graphite, as very available and cheap CM, has been published for the synthesis of quinoxalines from an extensive library of aromatic or aliphatic diamines and substituted 1,2-diketones, in EtOH, at room temperature, selectively leading to the corresponding quinoxalines in good-to-excellent yields (up to 71%) (Scheme 25).[131] Although it is not clear the participation of

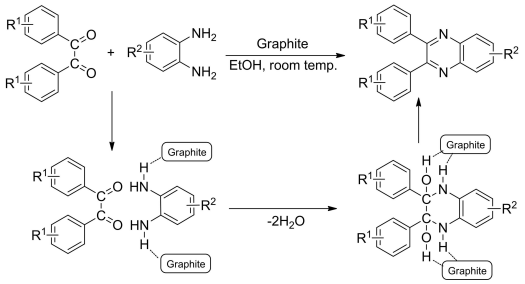

Scheme 25. Synthesis of quinoxalines from substituted-*o*-phenylendiamines and benzyls catalyzed by graphite.

graphite in the reaction, authors speculated about the formation of a cyclic intermediate by double-condensation which undergoes a double dehydration to yield quinoxalines. This hypothesis is reinforced by the fact that the formation of this intermediate compound was reported, although in low yields, when using commercially available Basolites – C-300, F-300 and Z-1200 –.[132]

As a modification of this approach, Roy et al.[133] reported an environmental-friendly methodology to successfully prepare quinoxalines from substituted 2-nitroanilines and benzyls, in the presence of GO, and using hydrazine as hydrogen donor. Since hydrazine reacts with benzyls, the reaction was carried out in two steps: i) complete reduction of nitro group in 2-nitroanilines to the corresponding diamines catalyzed by GO, in the presence of hydrazine, at 100 °C, and after cooling to 60 °C, ii) subsequent addition of the corresponding benzyl and to 80 °C when using the corresponding benzoin. Authors highlighted that the reaction can follow two different pathways: either sequential acid catalyzed reactions and subsequent final aromatization or alcohol oxidation from benzoin to benzyl, double-condensation with diamine and final dehydration.

Much more recently, Godino-Ojer et al.[82] reported an acid biomass-derived carbon from vegetal biomass catalyzing the quinoxalines synthesis in high conversions (98%, 4 h) and selectivity (83%), in toluene at 100 °C, under aerobic conditions, from *o*-phenylendiamine and benzoin. AC sample, showing a high developed porosity (S_{BET} = 2197 m^2/g and V_{pore} = 1.39 cm^3/g), was prepared from *Hedychium gardnerianum*, an invasive plant from Azores Islands, by chemical activation with H_3PO_4; the applied protocol allowed both the activation and simultaneous functionalization of the carbon surface comprising phosphorus-based functions. A combination of experimental results together a theoretical study, through DFT calculations, by selecting the most reduced models simulating the possible active centers in both phosphorylated ACs and others acid ACs functionalized with carboxylic or sulfonic functions allowed to conclude that the reaction probably occurs through the sequence: i) nucleophilic addition between reactants and subsequent dehydration, (ii) successive imine-enamine and keto-enol tautomerisms, (iii) heterocyclization and subsequent dehydration, and finally (iv) an aromatization step affording quinoxalines. In this case, the observed reactivity, in terms of conversion and selectivity, is probably governed by both the strength of the acid catalytic sites, but also by the textural properties. In the same context, a new set of transition metal-doped carbon gels (doped Fe, Co, Cu and Mo) were found to be active and selective in the synthesis of quinoxalines, under the experimental conditions referred above.[134] In this case, the metal phase, comprising metal oxides or zero-valent metals depending on the used metal and the carbonization temperature, and metal loading at the surface are determinant factors governing both reactivity and selectivity, the porosity barely influencing on the catalytic performance. The active catalytic sites are probably metal oxides although metal nanoparticles (Cu^0 or Co^0) could be involved in the last heterocyclic oxidative step. The influence of the surface chemistry was also investigated in such a manner that the additional presence of the OSGs in the Co-1000PO catalyst resulted on an enhancement of the catalytic performance probably due to the synergistic effect between both functions.

A most expensive but recyclable carbon-based catalyst, composed by CNT-supported Au nanoparticles, active in the synthesis of quinoxalines in high yields (up to 87% after 26–40 h), in a mixture of toluene/H_2O (1:1), at room temperature, from aromatic 1,2-diamines and α-hydroxy ketones or the corresponding 1,2-glycols, was designed by Shah et al.;[135] note that the presence of NaOH is required. In the same way, *N*-doped carbon supported Co[136] or Ru nanoparticle catalysts[137] have been reported for the acceptor-less dehydrogenation (ADC) cross-coupling of diamines with diols, in toluene at high temperature, to yield quinoxalines. Advantageously, Sun et al.[138] described the synthesis of advanced CMs based on *N,P* Co-doped cobalt catalyst (Co@NCP) derived from bimetallic (Co^{2+} and Zn^{2+}) ZIF for the synthesis of quinoxalines through ADC strategy from 2-nitroaniline and glycols, in the absence of any base, in toluene at 110–140 °C, exhibiting great catalytic performance (Scheme 26). The observed reactivity was attributed by one side to the high dispersion of Co nanoparticles at the carbon surface, but also to the formation of Co–P bonds, optimizing the coordination environment of the cobalt sites. It is noteworthy that the N and P doping increased the Lewis basicity in Co@NCP required for the dehydrogenation of glycols.

3.2.3. Pyrimidines and related compounds

One of the most studied syntheses of dihydropyrimidines (DHPMs) as biologically relevant medicinal scaffolds is MCR known as Biginelli condensation. Concerning to that, Safari et al[139] reported different MO_x supported on CNTs, where MO_x was TiO_2, MnO_2, Fe_3O_4, or NiO, as highly efficient catalysts for the synthesis of a great variety of DHPMs from aryl aldehydes, acetophenone and urea, under microwave irradiation at 90 °C, and in absence of any solvent (Scheme 27). Authors stablished the following reactivity order: TiO_2-MWCNTs > MnO_2-MWCNTs > Fe_3O_4-MWCNTs > NiO-MWCNTs, the best catalytic performance of TiO_2-MWCNTs being attributed to that titanium presents the greatest number of unoccupied *d*-orbitals resulting on the highest Lewis acidity. These catalysts were also applied to the synthesis of DHPMs by using distinct 1,3-dicarbonyl compounds under different reaction conditions.[140]

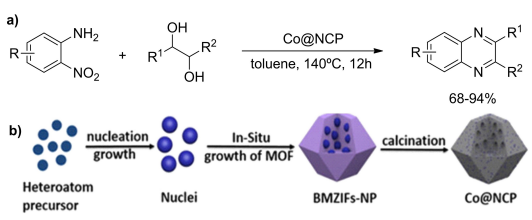

Scheme 26. (a) Synthesis of quinoxalines from 2-nitroaniline and glycols catalyzed by Co@NCP. (b) Synthesis scheme of Co@NCP (heteroatom precursor nucleate (ammonium phosphate). Reproduced from ref. [138] Copyright (2020), with permission from Wiley-VCH.

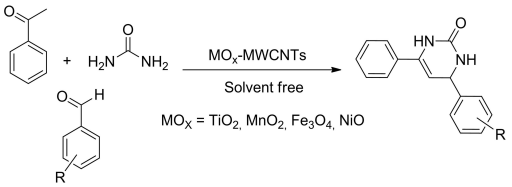

Scheme 27. Synthesis of DHPMs via Biginelli condensation catalyzed by TM metal oxides/MWCNTs.

Following a similar strategy a series of metal (M)–MWCNT nanocomposites (where M is Co, Pt, Cu or Ag) has been reported for the synthesis of dihydroquinazolinones by MCR between isatoic anhydride, primary amines or ammonium acetate with aromatic aldehydes, under ultrasound irradiation, at 35 kHz and 40 °C (Scheme 28).[141] The Co catalyst was found to be the most efficient one analyzing the catalyst amount (0.04 g) and the power of irradiation (pw = 70 W) selectively yielding the corresponding dihydroquinazolinone in 97% at 40 °C, after 6 min. MWCNTs decorated with Cu and Ag nanoparticles also resulted efficient catalysts for the synthesis of 2-aryl-2,3-dihydroquinazolin-4(1*H*)-ones by sonication of anthranilamide and different aldehydes.[142]

Ma et al.[143] developed a nanostructured iron catalyst (Fe–Fe_3C@NC-800), with hierarchically meso-, and microporosity, high S_{BET} and large V_{pore}, active in the oxidative coupling of amines and aldehydes, in water/THF, at 100 °C, in the presence of H_2O_2 as benign oxidant (Scheme 29). This CM was easily obtained by pyrolysis (800 °C) of a mixture of bamboo shoots, as *N*-containing biomass and iron salt mixture. Different iron phases including Fe^0 and Fe_3C nanoparticles beside Fe–N_x centers were contained in Fe–Fe_3C@NC-800 in such a manner that Fe^0 and Fe_3C form the core, which is covered by *N*-doped graphitic carbon layers showing coordinated Fe–N_x sites. Authors demonstrated that iron nanoparticles participate in the final aromatization step, the catalytic activity also increasing with Fe–N_x loading, observing a synergic effect for all iron species. In the same context, Song et al.[144] reported a highly dispersed Ni_2P nanoparticles on *N,P*-codoped biomass-derived porous carbon (Ni_2P@NPC-800) catalyzing the aerobic oxidative cross-dehydrogenative coupling of alcohols and diamines or even 2-aminobenzamides, in toluene at 120 °C, in this case

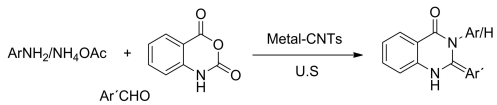

Scheme 28. Synthesis of substituted 2,3-dihydro-4(1*H*)-quinazolinones catalyzed by M–MWCNTs under sonication.

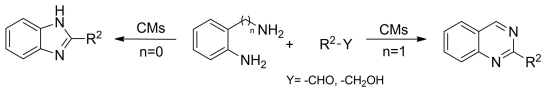

Scheme 29. Synthesis of quinazolines by in the oxidative coupling of amines and aldehydes or alcohols catalyzed by CMs.

requiring the presence of a base particularly *t*-BuOK, to obtain quinazolines in good-to-excellent yields (68–94%). This methodology was also successfully applied to the synthesis of benzimidazole when using o-phenylendiamine.

On the other side, Su et al.[145] prepared an active catalyst, composed by Co nanoparticles (as Co^0, Co^{3+}, Co–N_x, Co^{2+} species) encapsulated into *N,S* dual-doped CNT shells (Co@NSC-1), obtained by pyrolysis of a mixture of Co/Zn–ZIF-8 and thiourea at 900 °C. The catalyst was studied in the synthesis of quinazolinones from benzyl alcohol and 2-nitrobenzonitrile at 140 °C in absence of any additive (Scheme 30). In this case, the Zn^{2+} keeps away adjacent Co atoms while heteroatoms stabilizing Co nanoparticles. The synthesis of more complex ring-fused quinazolinones promoted by a MOF-derived Co nanocatalyst (Co-ZrO_2/N–C), from aminoarylmethanols and cyclic amines have been also reported.[146]

3.3. Seven-membered Rings

3.3.1. Benzodiazepines

Benzodiazepines are among the most prescribed drugs worldwide mainly by their psychotropic activity. Assuming that sulfated zirconia (SZr) is a widely used catalyst in industrial transformations, Godino-Ojer et al.[83] recently, published a new family of zirconia (Zr) and SZr/carbon composites active for the green synthesis of 2,3-dihydro-1*H*-1,5-benzodiazepines (Scheme 31). In this study, it was demonstrated that the Zr sample promotes the first reaction step to give the 2,3-

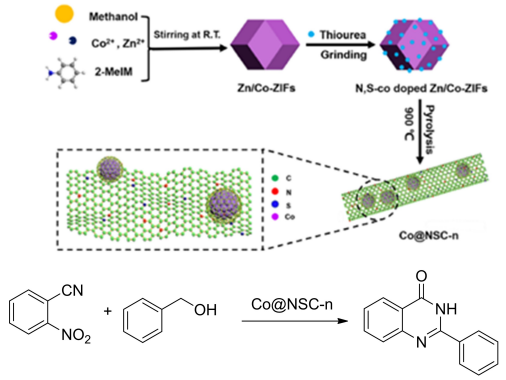

Scheme 30. Synthesis of quinazolinones by tandem hydrogen-transfer reaction between benzyl alcohol and 2-nitrobenzonitrile. Reproduced from ref. [146] Copyright (2022), with permission from American Chemical Society.

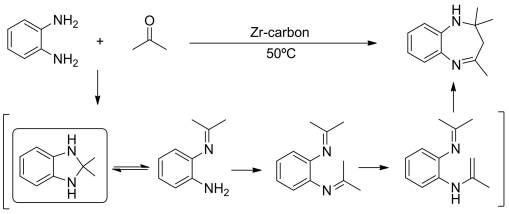

Scheme 31. Synthesis of benzodiazepines form *o*-phenylendiamines and acetone, at 50 °C, catalyzed by Zr and SZr/carbon composites.

dihydrobenzimidazole, while the Brönsted acid centers in SZr are involved in the final electrocyclization reaction affording the corresponding benzodiazepine. Interestingly, Zr or SZr-supported samples resulted more efficient catalysts than unsupported ones, even much more than other traditional acid catalysts (*e.g.* HY zeolite), giving benzodiazepine with quantitative conversion and total selectivity after 2 h (NZr–S1 sample).

In this way, the influence of both surface chemistry and porosity of carbon catalysts on catalytic performance has been also studied. At this regard, a series of recyclable metal-free porous carbon catalysts active in the synthesis of benzodiazepines has been published (Scheme 31).[84] Carbon catalysts, two of them commercially available – microporous Norit RX3 (NORIT Netherland B.V. and a xerogel mesoporous carbon (Xerolutions S.L.) – and a lab-prepared ordered mesoporous carbon, were oxidized with strong acids –HNO_3 or H_2SO_4–. This study allowed to conclude that both type and concentration of acid sites together with the porosity, particularly the microporosity, are key factors influencing on the observed reactivity. While acid catalytic sites such as –CO_2H functions enhanced the conversion values although decreasing the selectivity, the presence of –SO_3H groups at the carbon surface led to the corresponding benzodiazepine with lower conversion but total selectivity, reaching 90% of conversion after 2 h of reaction time when using N–S catalyst. In all the cases, microporosity was especially relevant affording the corresponding benzodiazepine with the highest selectivity. Although the carbon surface is also involved in the reaction, combination of both experimental and theoretical results, by using DFT calculations, demonstrated that the isomerization of 2,3-dihydrobenzimidazole intermediate to the corresponding monoimine is assisted by the presence of OSGs in catalysts also conditioned by the porosity of the CMs.

Munch more recently, spent tires were used to develop an acid carbon catalyst, obtained by chemical activation with H_3PO_4, promoting the synthesis of benzodiazepines with high conversion (83% after 2 h) and selectivity (84%).[85] Considering that the catalyst is a macroporous sample showing a large PSD enough to facilitate the diffusion of both reactants and products, the catalytic performance is mainly controlled by the chemical surface, specifically by the presence of phosphate groups at the edges of SiP_2O_7 supported phase or directly tethered at the carbon surface. In this case, theoretical results concerning the final cyclization step to benzodiazepines suggested that the most probable catalytic sites are phosphate functions in SiP_2O_7 although the participation of those directly anchored to the carbon surface could not be neglected.

4. Summary and Outlook

CMs are promising functional materials with multiple ecological applications in different domains which can contribute to a greener future.[147] These materials have been recognized during a long time as sustainable, versatile, and low-cost catalysts or catalysts supports with demonstrated efficiency in fine chemical synthesis, where the oldest and classical ACs are the most explored CMs.[11a] Nevertheless, a huge number of more recent carbon nanomaterials, such as CNTs, graphene derivatives or carbon gels, make that CMs gain much attention in catalysis.[148]

Catalytic performance mainly depends on different and varied factors such as the type and concentration of active sites, particularly the metal loading, and its distribution and dispersion, these last factors intimately related with the surface area and porosity. The versatility of CMs is based not only on the different nature of the carbon surface (sp^3, sp^2, *sp*-bonds) but also on the different morphology and the large number of post-modification methodologies reported to functionalize or modify the surface. Note that, doping of CMs with metals but also with foreign heteroatoms or even both, is a field in expansion and growing, providing materials with extraordinary stability and durability, and enhanced catalytic performances. Furthermore, the presence of structural defects and functional groups at the surface of CMs plays an important role to minimize metal aggregation and sintering, as well as specific interactions between the carbon surface and the target molecules. Therefore, the understanding and control of the surface chemistry on CMs, based on experimental but also theoretical knowledge, is a relevant issue of capital importance in the development of highly dispersed metal carbon-based catalysts and, hence, for catalyst design.

To the best of our knowledge, there is a lack of data concerning the industrial synthesis of *N*-heterocycles using carbon-based catalysts. However, in the fine chemical and pharmaceutical industries, several carbon-supported catalysts are frequently used in oxidation-reduction reactions. This preference is due to their extensive commercial availability (Ni, Pd, Pt or Cu/C, among the most popular) and the well-stablished experimental protocols for catalytic reactions. Certain carbon-based catalysts can be easily produced in high yields, exhibit both high thermal and chemical stability, can be recycled, and demonstrate both high activity and selectivity, all these factors directly impacting on economics. In fact, it is highly probable that in the near future, carbon catalysts will be industrially used for the synthesis of biologically significant *N*-heterocycles. Considering the mandatory green practices adopted by industries, N/P co-doped porous carbon (NPCH) catalysts were developed for the dehydrogenation of *N*-heterocycles to aromatic heterocycles on a gram scale and tolerating a great variability of functional groups,[149] as an example, could present a great potential to be used in industrial processes at a commercial level as alternative sustainable catalysts.

The small-size limit of metal particles supported on CMs still constitutes a challenge with increased interest. Current trends as new horizons for the CMs would comprise the development of SACs, still at the infancy, representing an excellent opportunity for the synthesis of heterocyclic systems, through cascade reactions, and offering great potential in terms of both high activity and selectivity. Efficiency of SACs in organic synthesis is already demonstrated, successfully being applied in relevant cross-coupling reactions such as Suzuki, Ullmann, Sonogashira, and Heck, to build C–C, and C-heteroatom bonds, advantageously offering sustainability of the processes due to the low metal content but also reducing the overall cost of the catalytic systems.[150] The main challenges to develop SACs

derived from CMs probably consist of the precise control of the coordination environments for metallic species besides the scalability and reproducibility. The enhancement of interactions between metallic species and the carbon support would allow the stabilization of metal particles, thereby mitigating the catalyst deactivation due to the metal leaching and sintering.

Structurally different CMs have been reported as catalysts active in the synthesis of a great variety of relevant *N*-containing heterocycles following diverse synthetic strategies, comprising mainly metal nanoparticles supported on distinct CMs. It is a reality that MOF-derived CMs, including SACs derived from MOFs, as well as heteroatom-doped graphenes, with optimized properties, present an extraordinary potential for the synthesis of valuable compounds, and specifically nitrogenated heterocycles, since just a few examples of these advanced carbon-based catalysts have been reported in this field.

Finally, earlier than later it will be possible the rational design of advanced carbon catalysts with application in fine chemical synthesis, a field with extraordinary industrial repercussion. To this end, both extensive experimental and theoretical studies including the synthesis and characterization of CMs but also their catalytic performance evaluation, addressed to stablish structure-activity relationships, are on the pyramid base to design catalysts with optimized properties. In this context, the understanding of the reaction mechanisms by computational methods (DFT calculations) will contribute to this progress, helping to identify the most probable catalytic sites from reduced models but also analyzing the preferred reaction pathways. In addition, the use of *operando* characterization techniques to gather information concerning driven catalysis measurements considering both the catalyst and the process, is crucial to optimize the reaction conditions and future rational design of new materials and molecules. Even in the future, machine learning (ML) techniques can be applied for the interpretation of large catalyst datasets to develop models and to generate new molecules studying the dynamics on catalyst surfaces and correlations between properties.[151]

Acknowledgements

This work has been supported by the Spanish Projects ref. PID2021-126579OB-C31 and PID2021-126579OB-C32 from MCIN/AEI/10.13039/501100011033 and "ERDF A way of making Europe, and UFV2023-38 from Universidad Francisco de Vitoria de Madrid. SMT acknowledges to MICIN/AEI/10.13039/501100011033 and FSE "El FSE invierte en tu futuro" for the Ramon y Cajal research contract.

Conflict of Interests

The authors declare no conflict of interest.

Keywords: Porous carbons · Catalysts · Green Chemistry · Fine chemicals · Heterocycles

[1] a) C. H. Collett, J. McGregor, *Catal. Sci. Technol.* **2016**, *6*, 363–378; b) F. J. Maldonado-Hodar, L. M. P. Madeira, M. F. Portela, *J. Catal.* **1996**, *164*, 399–410.
[2] a) V. Calvino-Casilda, A. J. Lopez-Peinado, C. J. Duran-Valle, R. M. Martin-Aranda, *Catal. Rev. Sci. Eng.* **2010**, *52*, 325–380; b) F. J. Maldonado-Hodar, *Catal. Today* **2013**, *218–219*, 43–50; c) F. Rodriguez-Reinoso, *Carbon* **1998**, *36*, 159–175.
[3] a) R. Bogdanowicz, *Curr. Opin. Solid State Mater. Sci.* **2022**, *26*, 100991; b) M. B. R. Burkholder, F. B. Rahman, E. Chandler Jr., J. R. Regalbuto, B. F. Gupton, J. Meynard, M. Tengco, *Carbon Trends* **2022**, *9*, 100196–100214; c) M. Li, Z. W. Li, Q. Lin, J. X. Cao, F. Liu, S. Kawi, *Chem. Eng. J.* **2022**, *431*, 133970; d) F. J. Maldonado-Hódar, C. Moreno-Catila, J. Rivera-Utrilla, M. A. Ferro-Garcia, *Stud. Surf. Sci. Catal.* **2000**, *130*, 1107–1112.
[4] a) C. Moreno-Castilla, M. V. Lopez-Ramon, F. Carrasco-Marin, *Carbon* **2000**, *38*, 1995–2001; b) F. Rodriguez Reinoso, M. Molina-Sabio, *Carbon* **1992**, *30*, 1111–1118.
[5] R. E. Franklin, *Proc. R. Soc. A: Math. Phys. Eng. Sci.* **1951**, *209*, 196–218.
[6] A. Krueger, *Carbon Materials and Nanotechnology*, WILEY-VCH Weinheim, **2010**.
[7] a) A. Bianco, H.-M. Cheng, T. Enoki, Y. Gogotsi, R. H. Hurt, N. Koratkar, T. Kyotani, M. Monthioux, C. R. Park, J. M. D. Tascon, J. Zhang, *Carbon* **2013**, *65*, 1–6; b) N. S. Kasalkova, P. Slepicka, V. Svorcik, *Nanomaterials* **2021**, *11*, 2368; c) S. Li, L. Li, H. Y. Tu, H. Zhang, D. S. Silvester, C. E. Banks, G. Q. Zou, H. S. Hou, X. B. Ji, *Mater. Today* **2021**, *51*, 188–207; d) D. K. Rajak, A. Kumar, A. Behera, P. L. Menezes, *Appl. Sci.* **2021**, *11*, 4445.
[8] a) C. Lamberth, J. Dinges, *Bioactive Heterocyclic Compound Classes: Agrochemicals*, Wiley-VCH Verlag GmbH & Co. KGaA., Weinheim, Germany, **2012**; b) A. V. Iosub, S. S. Stahl, *Org. Lett.* **2015**, *17*, 4404–4407.
[9] A. Mohammad, Inamuddin, *Green Solvents I: Properties and Applications in Chemistry*, Springer, New York, **2012**.
[10] a) N. Bugday, S. Altin, S. Yasar, *Appl. Organomet. Chem.* **2021**, *35*; b) A. Jackowski, S. I. Zones, S. J. Hwang, A. W. Burton, *J. Am. Chem. Soc.* **2009**, *131*, 1092–1100; c) T. Toyao, M. Fujiwaki, K. Miyahara, T. H. Kim, Y. Horiuchi, M. Matsuoka, *ChemSusChem* **2015**, *8*, 3905–3912; d) Y. Li, Q. Shao, H. He, C. Zhu, X. S. Xue, J. Xie, *Nat. Commun.* **2022**, *13*, 10.
[11] a) E. Pérez-Mayoral, V. Calvino-Casilda, E. Soriano, *Catal. Sci. Technol.* **2016**, *6*, 1265–1291; b) E. Pérez Mayoral, M. Godino Ojer, M. Ventura, I. Matos, *Nanomaterials* **2023**, *13*, 2013.
[12] a) E. Perez-Mayoral, I. Matos, M. Bernardo, I. M. Fonseca, *Catalysts* **2019**, *9*, 133; b) J. Wang, Y. L. Wang, H. B. Hu, Q. P. Yang, J. J. Cai, *Nanoscale* **2020**, *12*, 4238–4268; c) E. Pérez-Mayoral, M. Godino-Ojer, I. Matos, M. Bernardo, *Catalysts* **2023**, *13*, 541.
[13] a) V. Hasija, S. Patial, P. Raizada, A. A. P. Khan, A. M. Asiri, Q. V. Le, V. H. Nguyen, P. Singh, *Coord. Chem. Rev.* **2022**, *452*, 214298; b) H. Huang, K. Shen, F. Chen, Y. Li, *ACS Catal.* **2020**, *10*, 6579–6586.
[14] X. F. Yang, A. Q. Wang, B. T. Qiao, J. Li, J. Y. Liu, T. Zhang, *Acc. Chem. Res.* **2013**, *46*, 1740–1748.
[15] P. Ehrburger, F. Louys, J. Lahaye, *Carbon* **1989**, *27*, 389–393.
[16] A. Das, S. Mondal, K. M. Hansda, M. K. Adak, D. Dhak, *Appl. Catal. A* **2023**, *649*, 118955.
[17] a) N. Z. M. Azmi, A. Buthiyappan, A. A. A. Raman, M. F. A. Patah, S. Sufian, *J. Ind. Eng. Chem.* **2022**, *116*, 1–20; b) R. Bhattacharya, *J. Environ. Manage.* **2023**, *325*, 116613.
[18] A. Bacaoui, A. Dahbi, A. Yaacoubi, C. Bennouna, F. J. Maldonado-Hodar, J. Rivera-Utrilla, F. Carrasco-Marin, C. Moreno-Castilla, *Environ. Sci. Technol.* **2002**, *36*, 3844–3849.
[19] J. L. Figueiredo, M. F. R. Pereira, *Catal. Today* **2010**, *150*, 2–7.
[20] J. F. Vivo-Vilches, E. Bailon-Garcia, A. F. Perez-Cadenas, F. Carrasco-Marin, F. J. Maldonado-Hodar, *Carbon* **2014**, *68*, 520–530.
[21] F. J. Maldonado-Hodar, A. F. Perez-Cadenas, J. L. G. Fierro, C. Moreno-Castilla, *J. Phys. Chem. B* **2003**, *107*, 5003–5007.
[22] Y. L. Cao, S. J. Mao, M. M. Li, Y. Q. Chen, Y. Wang, *ACS Catal.* **2017**, *7*, 8090–8112.
[23] S. T. Tibor, C. A. Grande, *Clean. Eng. Technol.* **2022**, *7*, 100443–100451.
[24] a) P. Bayer, E. Heuer, U. Karl, M. Finkel, *Water Res.* **2005**, *39*, 1719–1728; b) A. Vilen, P. Laurell, R. Vahala, *J. Environ. Manage.* **2022**, *324*, 116356.
[25] a) S. Iijima, *Nature* **1991**, *354*, 56–58; b) S. Iijima, T. Ichihashi, *Nature* **1993**, *363*, 603–605.

[26] J. P. Tessonnier, D. S. Su, *ChemSusChem* **2011**, *4*, 824–847.
[27] R. Andrews, D. Jacques, D. L. Qian, T. Rantell, *Acc. Chem. Res.* **2002**, *35*, 1008–1017.
[28] R. D. Gately, M. I. H. Panhuis, *Beilstein J. Nanotechnol.* **2015**, *6*, 508–516.
[29] a) M. V. Kharlamova, M. Paukov, M. G. Burdanova, *Materials* **2022**, *15*, 24; b) M. V. Qanati, A. Rasooli, *Diam. Relat. Mat.* **2020**, *109*, 108097.
[30] S. Panic, A. Kukovecz, G. Boskovic, *Appl. Catal. B* **2018**, *225*, 207–217.
[31] Z. J. Li, G. Li, X. L. Chen, Z. Xia, B. Yang, J. N. Yao, L. C. Lei, Y. Hou, *ChemSusChem* **2018**, *11*, 2382–2387.
[32] a) S. C. Tsang, P. J. F. Harris, M. L. H. Green, *Nature* **1993**, *362*, 520–522; b) D. B. Mawhinney, V. Naumenko, A. Kuznetsova, J. T. Yates, J. Liu, R. E. Smalley, *J. Am. Chem. Soc.* **2000**, *122*, 2383–2384.
[33] S. Morales-Torres, F. J. Maldonado-Hodar, A. F. Perez-Cadenas, F. Carrasco-Marin, *J. Hazard. Mater.* **2010**, *183*, 814–822.
[34] S. Morales-Torres, T. L. Silva, L. M. Pastrana-Martinez, A. T. Brandao, J. L. Figueiredo, A. M. Silva, *Phys. Chem. Chem. Phys.* **2014**, *16*, 12237–12250.
[35] a) I. D. Rosca, F. Watari, M. Uo, T. Akasaka, *Carbon* **2005**, *43*, 3124–3131; b) Martınez, M. A. Callejas, A. M. Benito, M. Cochet, T. Seeger, A. Ansón, J. Schreiber, C. Gordon, C. Marhic, O. Chauvet, J. L. G. Fierro, W. K. Maser, *Carbon* **2003**, *41*, 2247–2256; c) C. G. Salzmann, S. A. Llewellyn, G. Tobias, M. A. H. Ward, Y. Huh, M. L. H. Green, *Adv. Mater.* **2007**, *19*, 883–887.
[36] F. Avilés, J. V. Cauich-Rodríguez, L. Moo-Tah, A. May-Pat, R. Vargas-Coronado, *Carbon* **2009**, *47*, 2970–2975.
[37] S. Hanelt, G. Orts-Gil, J. F. Friedrich, A. Meyer-Plath, *Carbon* **2011**, *49*, 2978–2988.
[38] a) K. J. Ziegler, Z. Gu, H. Peng, E. L. Flor, R. H. Hauge, R. E. Smalley, *J. Am. Chem. Soc.* **2005**, *127*, 1541–1547; b) V. Datsyuk, M. Kalyva, K. Papagelis, J. Parthenios, D. Tasis, A. Siokou, I. Kallitsis, C. Galiotis, *Carbon* **2008**, *46*, 833–840.
[39] J. Chen, Q. Chen, Q. Ma, *J. Colloid Interface Sci.* **2012**, *370*, 32–38.
[40] S. W. Kim, T. Kim, Y. S. Kim, H. S. Choi, H. J. Lim, S. J. Yang, C. R. Park, *Carbon* **2012**, *50*, 3–33.
[41] K. S. Novoselov, A. K. Geim, S. V. Morozov, D. Jiang, Y. Zhang, S. V. Dubonos, I. V. Grigorieva, A. A. Firsov, *Science* **2004**, *306*, 666–669.
[42] a) C. Botas, P. Álvarez, P. Blanco, M. Granda, C. Blanco, R. Santamaría, L. J. Romasanta, R. Verdejo, M. A. López-Manchado, R. Menéndez, *Carbon* **2013**, *65*, 156–164; b) W. S. Hummers, R. E. Offeman, *J. Am. Chem. Soc.* **2002**, *80*, 1339–1339; c) B. C. Brodie, *Ann. Chim. Phys.* **1860**, *59*, 466–472.
[43] a) L. M. Pastrana-Martínez, S. Morales-Torres, V. Likodimos, J. L. Figueiredo, J. L. Faria, P. Falaras, A. M. T. Silva, *Appl. Catal. B* **2012**, *123–124*, 241–256; b) S. Morales-Torres, L. M. Pastrana-Martinez, J. L. Figueiredo, J. L. Faria, A. M. Silva, *Environ. Sci. Pollut. Res. Int.* **2012**, *19*, 3676–3687.
[44] H. A. Becerril, J. Mao, Z. Liu, R. M. Stoltenberg, Z. Bao, Y. Chen, *ACS Nano* **2008**, *2*, 463–470.
[45] L. M. Pastrana-Martínez, S. Morales-Torres, V. Likodimos, P. Falaras, J. L. Figueiredo, J. L. Faria, A. M. T. Silva, *Appl. Catal. B* **2014**, *158–159*, 329–340.
[46] L. B. Hu, X. R. Hu, X. B. Wu, C. L. Du, Y. C. Dai, J. B. Deng, *Physica B+C* **2010**, *405*, 3337–3341.
[47] Z. Cheng, R. F. Wang, Y. Wang, Y. S. Cao, Y. X. Shen, Y. Huang, Y. S. Chen, *Carbon* **2023**, *205*, 112–137.
[48] R. Z. Wan, C. Y. Wang, R. Chen, M. Liu, F. Yang, *Int. J. Hydrogen Energy* **2022**, *47*, 32039–32049.
[49] a) L. M. Pastrana-Martínez, S. Morales-Torres, S. K. Papageorgiou, F. K. Katsaros, G. E. Romanos, J. L. Figueiredo, J. L. Faria, P. Falaras, A. M. T. Silva, *Appl. Catal. B* **2013**, *142–143*, 101–111; b) S. Morales-Torres, L. M. Pastrana-Martínez, J. L. Figueiredo, J. L. Faria, A. M. T. Silva, *Appl. Surf. Sci.* **2013**, *275*, 361–368; c) A. Perez-Molina, S. Morales-Torres, F. J. Maldonado-Hodar, L. M. Pastrana-Martinez, *Nanomaterials* **2020**, *10*, 1106; d) N. Mirikaram, A. Perez-Molina, S. Morales-Torres, A. Salemi, F. J. Maldonado-Hodar, L. M. Pastrana-Martinez, *Nanomaterials* **2021**, *11*, 1576; e) L. T. Pérez-Poyatos, L. M. Pastrana-Martínez, S. Morales-Torres, P. Sánchez-Moreno, M. Bramini, F. J. Maldonado-Hódar, *Catal. Today* **2023**, DOI: 10.1016/j.cattod.2023.01.017.
[50] a) C. P. Athanasekou, S. Morales-Torres, V. Likodimos, G. E. Romanos, L. M. Pastrana-Martinez, P. Falaras, D. D. Dionysiou, J. L. Faria, J. L. Figueiredo, A. M. T. Silva, *Appl. Catal. B* **2014**, *158*, 361–372; b) L. M. Pastrana-Martinez, S. Morales-Torres, J. L. Figueiredo, J. L. Faria, A. M. T. Silva, *Water Res.* **2015**, *77*, 179–190.
[51] Y. N. Hu, D. X. Hao, F. L. Gong, Y. Y. Gao, X. R. Yan, G. H. Ma, *Particuology* **2021**, *56*, 33–42.
[52] S. S. Kistler, *Nature* **1931**, *127*, 741–741.
[53] R. W. Pekala, *J. Mater. Sci.* **1989**, *24*, 3221–3227.
[54] R. W. Pekala, N° Patent: 4997804, **1991**.
[55] H. Jirglova, A. F. Perez-Cadenas, F. J. Maldonado-Hodar, *Langmuir* **2009**, *25*, 2461–2466.
[56] S. J. Han, Q. F. Sun, H. H. Zheng, J. P. Li, C. D. Jin, *Carbohydr. Polym.* **2016**, *136*, 95–100.
[57] S. A. Al-Muhtaseb, J. A. Ritter, *Adv. Mater.* **2003**, *15*, 101–114.
[58] a) O. Czakkel, K. Marthi, E. Geissler, K. Laszlo, *Microporous Mesoporous Mater.* **2005**, *86*, 124–133; b) N. Job, A. Thery, R. Pirard, J. Marien, L. Kocon, J. N. Rouzaud, F. Beguin, J. P. Pirard, *Carbon* **2005**, *43*, 2481–2494.
[59] R. Kocklenberg, B. Mathieu, S. Blacher, R. Pirard, J. P. Pirard, R. Sobry, G. Van den Bossche, *J. Non-Cryst. Solids* **1998**, *225*, 8–13.
[60] E. Gallegos-Suarez, A. F. Perez-Cadenas, F. J. Maldonado-Hodar, F. Carrasco-Marin, *Chem. Eng. J.* **2012**, *181*, 851–855.
[61] C. Lin, J. A. Ritter, *Carbon* **1997**, *35*, 1271–1278.
[62] C. Lin, J. A. Ritter, *Carbon* **2000**, *38*, 849–861.
[63] L. Zubizarreta, A. Arenillas, J. P. Pirard, J. J. Pis, N. Job, *Microporous Mesoporous Mater.* **2008**, *115*, 480–490.
[64] M. Godino-Ojer, E. Soriano, V. Calvino-Casilda, F. J. Maldonado-Hodar, E. Perez-Mayoral, *Chem. Eng. J.* **2017**, *314*, 488–497.
[65] F. J. Maldonado-Hodar, M. A. Ferro-Garcia, J. Rivera-Utrilla, C. Moreno-Castilla, *Carbon* **1999**, *37*, 1199–1205.
[66] a) F. J. Maldonado-Hodar, C. Moreno-Castilla, A. F. Perez-Cadenas, *Microporous Mesoporous Mater.* **2004**, *69*, 119–125; b) F. J. Maldonado-Hódar, C. Moreno-Castilla, J. Rivera-Utrilla, Y. Hanzawa, Y. Yamada, *Langmuir* **2000**, *16*, 4367–4373.
[67] L. Song, T. W. Xue, Z. C. Shen, S. L. Yang, D. T. Sun, J. Yang, Y. Z. Hong, Y. Z. Su, H. T. Wang, L. Peng, J. Li, *J. Colloid Interface Sci.* **2022**, *621*, 398–405.
[68] L. N. Zhang, J. Zhang, G. F. Wang, W. T. Zhao, J. G. Chen, *J. Fuel Chem. Technol.* **2022**, *50*, 1331–1340.
[69] C. Alegre, M. E. Galvez, E. Baquedano, E. Pastor, R. Moliner, M. J. Lazaro, *Int. J. Hydrogen Energy* **2012**, *37*, 7180–7191.
[70] F. J. Maldonado-Hódar, H. Jirglová, S. Morales-Torres, A. F. Pérez-Cadenas, *Catal. Today* **2018**, *301*, 217–225.
[71] S. Morales-Torres, H. Jirglova, L. M. Pastrana-Martinez, F. J. Maldonado-Hodar, *Processes* **2020**, *8*, 746.
[72] a) F. J. Maldonado-Hodar, S. Morales-Torres, F. Ribeiro, E. R. Silva, A. F. Perez-Cadenas, F. Carrasco-Marin, F. A. C. Oliveira, *Langmuir* **2008**, *24*, 3267–3273; b) S. Morales-Torres, F. J. Maldonado-Hódar, A. F. Pérez-Cadenas, F. Carrasco-Marín, *Microporous Mesoporous Mater.* **2012**, *153*, 24–29.
[73] a) F. J. Maldonado-Hodar, C. Moreno-Castilla, J. Rivera-Utrilla, *Appl. Catal. A* **2000**, *203*, 151–159; b) C. Moreno-Castilla, F. J. Maldonado-Hodar, *Phys. Chem. Chem. Phys.* **2000**, *2*, 4818–4822.
[74] H. Hamad, E. Bailon-Garcia, A. F. Perez-Cadenas, F. J. Maldonado-Hodar, F. Carrasco-Marin, *J. Environ. Chem. Eng.* **2020**, *8*, 104350.
[75] H. H. Cao, J. D. Cao, F. H. Wang, H. Zhu, M. Pu, *Electrochim. Acta* **2020**, *333*, 135560.
[76] S. Morales-Torres, F. Carrasco-Marin, A. F. Perez-Cadenas, F. J. Maldonado-Hodar, *Catalysts* **2015**, *5*, 774–799.
[77] a) M. Godino-Ojer, A. J. Lopez-Peinado, F. J. Maldonado-Hodar, E. Bailon-Garcia, E. Perez-Mayoral, *Dalton Trans.* **2019**, *48*, 5637–5648; b) M. Godino-Ojer, S. Morales-Torres, E. Perez-Mayoral, F. J. Maldonado-Hodar, *J. Environ. Chem. Eng.* **2022**, *10*, 106879.
[78] J. B. Donnet, *Carbon* **1968**, *6*, 161–176.
[79] Y. Sun, C. Cao, C. Liu, J. Liu, Y. Zhu, X. Wang, W. Song, *Carbon* **2017**, *125*, 139–145.
[80] A. Gervasini, A. Auroux, *J. Catal.* **1991**, *131*, 190–198.
[81] F. Carrasco-Marín, A. Mueden, C. Moreno-Castilla, *J. Phys. Chem. B* **1998**, *102*, 9239–9244.
[82] M. Godino-Ojer, R. Blazquez-Garcia, I. Matos, M. Bernardo, I. M. Fonseca, E. P. Mayoral, *Catal. Today* **2020**, *354*, 90–99.
[83] M. Godino-Ojer, L. Milla-Diez, I. Matos, C. J. Duran-Valle, M. Bernardo, I. M. Fonseca, E. P. Mayoral, *ChemCatChem* **2018**, *10*, 5215–5223.
[84] M. Godino-Ojer, I. Matos, M. Bernardo, R. Carvalho, O. Soares, C. Duran-Valle, I. M. Fonseca, E. P. Mayoral, *Catal. Today* **2020**, *357*, 64–73.
[85] M. Godino-Ojer, V. R. Morales, A. J. L. Peinado, M. Bernardo, N. Lapa, A. M. Ferraria, A. M. B. do Rego, I. M. Fonseca, I. Matos, E. Perez-Mayoral, *Catal. Today* **2023**, *419*, 114160.
[86] A. Rai, K. V. S. Ranganath, *J. Heterocycl. Chem.* **2021**, *58*, 1039–1057.
[87] T. W. van Deelen, C. Hernández Mejía, K. P. de Jong, *Nat. Catal.* **2019**, *2*, 955–970.

[88] Z. Chen, Z. Guan, M. Li, Q. Yang, C. Li, *Angew. Chem. Int. Ed.* **2011**, *50*, 4913–4917.
[89] Z. Dağalan, H. Can, A. Daştan, B. Nişancı, Ö. Metin, *Tetrahedron* **2022**, *114*, 132766.
[90] X. Yu, R. Nie, H. Zhang, X. Lu, D. Zhou, Q. Xia, *Microporous Mesoporous Mater.* **2018**, *256*, 10–17.
[91] J. Zhang, S. Chen, F. Chen, W. Xu, G.-J. Deng, H. Gong, *Adv. Synth. Catal.* **2017**, *359*, 2358–2363.
[92] E. Ruijter, R. V. A. Orru, *Drug Discovery Today Technol.* **2013**, *10*, 15–20.
[93] Z. Gong, Y. Lei, P. Zhou, Z. H. Zhang, *New J. Chem.* **2017**, *41*, 10613–10618.
[94] P. Zhou, L. Jiang, F. Wang, K. J. Deng, K. L. Lv, Z. H. Zhang, *Sci. Adv.* **2017**, *3*, e1601945.
[95] S. Siddiki, A. S. Touchy, C. Chaudhari, K. Kon, T. Toyao, K. Shimizu, *Org. Chem. Front.* **2016**, *3*, 846–851.
[96] M. Gruber, S. Chouzier, K. Koehler, L. Djakovitch, *Appl. Catal. A* **2004**, *265*, 161–169.
[97] M. J. Albaladejo, F. Alonso, M. Yus, *Chem. Eur. J.* **2013**, *19*, 5242–5245.
[98] M. Krivec, M. Gazvoda, K. Kranjc, S. Polanc, M. Kocevar, *J. Org. Chem.* **2012**, *77*, 2857–2864.
[99] H. Sharghi, J. Aboonajmi, M. Mozaffari, M. M. Doroodmand, M. Aberi, *Appl. Organomet. Chem.* **2018**, *32*, e4124.
[100] M. Zakeri, E. Abouzari-lotf, M. Miyake, S. Mehdipour-Ataei, K. Shameli, *Arab. J. Chem.* **2019**, *12*, 188–197.
[101] S. Kumari, A. Shekhar, D. D. Pathak, *New J. Chem.* **2016**, *40*, 5053–5060.
[102] H. D. Hanoon, E. Kowsari, M. Abdouss, M. H. Ghasemi, H. Zandi, *Res. Chem. Intermed.* **2017**, *43*, 4023–4041.
[103] X. Guo, J. A. Shao, H. Liu, B. H. Chen, W. T. Chen, Y. P. Yu, *RSC Adv.* **2015**, *5*, 51559–51562.
[104] H. Ghafuri, M. Talebi, *Ind. Eng. Chem. Res.* **2016**, *55*, 2970–2982.
[105] N. A. Weires, J. Boster, J. Magolan, *Eur. J. Org. Chem.* **2012**, *2012*, 6508–6512.
[106] C. C. Lin, W. H. Wan, X. T. Wei, J. Z. Chen, *ChemSusChem* **2021**, *14*, 709–720.
[107] M. Shaikh, R. Yadav, P. K. Tyagi, L. Mishra, K. V. S. Ranganath, *ChemNanoMat* **2018**, *4*, 542–545.
[108] S. G. Agalave, S. R. Maujan, V. S. Pore, *Chem. Asian J.* **2011**, *6*, 2696–2718.
[109] B. H. Lipshutz, B. R. Taft, *Angew. Chem. Int. Ed.* **2006**, *45*, 8235–8238.
[110] C. T. Lee, S. L. Huang, B. H. Lipshutz, *Adv. Synth. Catal.* **2009**, *351*, 3139–3142.
[111] a) F. Alonso, Y. Moglie, G. Radivoy, M. Yus, *Adv. Synth. Catal.* **2010**, *352*, 3208–3214; b) F. Alonso, Y. Moglie, G. Radivoy, M. Yus, *Org. Biomol. Chem.* **2011**, *9*, 6385–6395.
[112] A. S. Nia, S. Rana, D. Dohler, X. Noirfalise, A. Belfiore, W. H. Binder, *Chem. Commun.* **2014**, *50*, 15374–15377.
[113] Z. F. Li, H. Y. Zhao, H. T. Han, J. Y. Song, Y. Liu, W. H. Guo, Z. Z. Sun, W. Y. Chu, *Appl. Organomet. Chem.* **2018**, *32*, 9.
[114] a) H. Naeimi, Z. Ansarian, *Inorg. Chim. Acta* **2017**, *466*, 417–425; b) H. Naeimi, R. Shaabani, *Ultrason. Sonochem.* **2017**, *34*, 246–254.
[115] N. Salam, A. Sinha, A. S. Roy, P. Mondal, N. R. Jana, S. M. Islam, *RSC Adv.* **2014**, *4*, 10001–10012.
[116] C. Rossy, J. Majimel, M. T. Delapierre, E. Fouquet, F. X. Felpin, *J. Organomet. Chem.* **2014**, *755*, 78–85.
[117] I. Yamane, K. Sato, R. Otomo, T. Yanase, A. Miura, T. Nagahama, Y. Kamiya, T. Shimada, *Nanomaterials* **2021**, *11*, 10.
[118] Z. Z. Wang, X. H. Zhou, S. F. Gong, J. W. Xie, *Nanomaterials* **2022**, *12*, 1070.
[119] G. Qi, W. G. Zhang, Y. Dai, *Res. Chem. Intermed.* **2015**, *41*, 1149–1155.
[120] M. Nasrollahzadeh, B. Jaleh, A. Jabbari, *RSC Adv.* **2014**, *4*, 36713–36720.
[121] Y. Yildiz, I. Esirden, E. Erken, E. Demir, M. Kaya, F. Sen, *ChemistrySelect* **2016**, *1*, 1695–1701.
[122] N. Basavegowda, K. Mishra, Y. R. Lee, *Mater. Technol.* **2019**, *34*, 558–569.
[123] Z. Zarnegar, J. Safari, Z. M. Kafroudi, *New J. Chem.* **2015**, *39*, 1445–1451.
[124] B. Aday, H. Pamuk, M. Kaya, F. Sen, *J. Nanosci. Nanotechnol.* **2016**, *16*, 6498–6504.
[125] J. Lopez-Sanz, E. Perez-Mayoral, E. Soriano, D. Omenat-Moran, C. J. Duran, R. M. Martin-Aranda, I. Matos, I. Fonseca, *ChemCatChem* **2013**, *5*, 3736–3742.
[126] J. Marco-Contelles, E. Perez-Mayoral, A. Samadi, M. D. Carreiras, E. Soriano, *Chem. Rev.* **2009**, *109*, 2652–2671.
[127] M. Godino-Ojer, A. J. López-Peinado, F. J. Maldonado-Hódar, E. Pérez-Mayoral, *ChemCatChem* **2017**, *9*, 1422–1428.
[128] M. Godino-Ojer, R. M. Martín-Aranda, F. J. Maldonado-Hódar, A. F. Pérez-Cadenas, E. Pérez-Mayoral, *J. Mol. Catal.* **2018**, *445*, 223–231.
[129] M. Godino-Ojer, A. J. Lopez-Peinado, R. M. Martin-Aranda, J. Przepiorski, E. Perez-Mayoral, E. Soriano, *ChemCatChem* **2014**, *6*, 3440–3447.
[130] Z. Chen, J. Song, X. Peng, S. Xi, J. Liu, W. Zhou, R. Li, R. Ge, C. Liu, H. Xu, X. Zhao, H. Li, X. Zhou, L. Wang, X. Li, L. Zhong, A. I. Rykov, J. Wang, M. J. Koh, K. P. Loh, *Adv. Mater.* **2021**, *33*, e2101382.
[131] H. K. Kadam, S. Khan, R. A. Kunkalkar, S. G. Tilve, *Tetrahedron Lett.* **2013**, *54*, 1003–1007.
[132] M. Godino-Ojer, M. Shamzhy, J. Cejka, E. Perez-Mayoral, *Catal. Today* **2020**, *345*, 258–266.
[133] B. L. Roy, S. Ghosh, P. Ghosh, B. Basu, *Tetrahedron Lett.* **2015**, *56*, 6762–6767.
[134] M. Godino-Ojer, S. Morales-Torres, F. J. Maldonado-Hódar, E. Pérez-Mayoral, *Catal. Today* **2023**, DOI: 10.1016/j.cattod.2023.01.021.
[135] N. Shah, E. Gravel, D. V. Jawale, E. Doris, I. N. N. Namboothiri, *ChemCatChem* **2015**, *7*, 57–61.
[136] D. Panja, B. Paul, B. Balasubramaniam, R. K. Gupta, S. Kundu, *Catal. Commun.* **2020**, *137*, 105927.
[137] B. Guo, H. X. Li, S. Q. Zhang, D. J. Young, J. P. Lang, *ChemCatChem* **2018**, *10*, 5627–5636.
[138] K. K. Sun, D. D. Li, G. P. Lu, C. Cai, *ChemCatChem* **2021**, *13*, 373–381.
[139] J. Safari, S. Gandomi-Ravandi, *J. Mol. Struct.* **2014**, *1074*, 71–78.
[140] a) J. Safari, Z. Zarnegar, *RSC Adv.* **2013**, *3*, 17962–17967; b) J. Safari, S. Gandomi-Ravandi, *J. Iran. Chem. Soc.* **2015**, *12*, 147–154; c) J. Safari, S. Gandomi-Ravandi, *New J. Chem.* **2014**, *38*, 3514–3521; d) J. Safari, S. Gandomi-Ravandi, *J. Mol. Catal. A* **2013**, *373*, 72–77.
[141] J. Safari, S. Gandomi-Ravandi, *J. Mol. Struct.* **2014**, *1072*, 173–178.
[142] a) J. Safari, S. Gandomi-Ravandi, *RSC Adv.* **2014**, *4*, 11654–11660; b) J. Safari, S. Gandomi-Ravandi, *J. Mol. Catal. A* **2013**, *371*, 135–140.
[143] Z. M. Ma, T. Song, Y. Z. Yuan, Y. Yang, *Chem. Sci.* **2019**, *10*, 10653–10653.
[144] T. Song, P. Ren, Z. M. Ma, J. L. Xiao, Y. Yang, *ACS Sustainable Chem. Eng.* **2020**, *8*, 267–277.
[145] T. Y. Su, K. K. Sun, G. P. Lu, C. Cai, *ACS Sustainable Chem. Eng.* **2022**, *10*, 3872–3881.
[146] F. Xie, Q. H. Chen, R. Xie, H. F. Jiang, M. Zhang, *ACS Catal.* **2018**, *8*, 5869–5874.
[147] K. P. Gopinath, D.-V. N. Vo, D. Gnana Prakash, A. Adithya Joseph, S. Viswanathan, J. Arun, *Environ. Chem. Lett.* **2020**, *19*, 557–582.
[148] a) A. Sharma, S. Gudala, S. R. Ambati, S. Penta, S. P. Mahapatra, R. R. Vedula, S. Pola, B. Acharya, *J. Chin. Chem. Soc.* **2017**, *64*, 589–606; b) A. Rai, K. V. S. Ranganath, *J. Heterocycl. Chem.* **2020**, *58*, 1039–1057; c) Y. Cheng, Y. Fan, Y. Pei, M. Qiao, *Catal. Sci. Technol.* **2015**, *5*, 3903–3916; d) Y. Ito, Y. Hari, *Chem. Rec.* **2022**, *22*, e202100325.
[149] K. Sun, H. Shan, R. Ma, P. Wang, H. Neumann, G.-P. Lu, M. Beller, *Chem. Sci.* **2022**, *13*, 6865–6872.
[150] V. B. Saptal, V. Ruta, M. A. Bajada, G. Vile, *Angew. Chem. Int. Ed.* **2023**, *n/a*, e202219306.
[151] J. R. Kitchin, *Nat. Catal.* **2018**, *1*, 230–232.

Manuscript received: July 28, 2023
Revised manuscript received: October 16, 2023
Accepted manuscript online: October 16, 2023
Version of record online: November 22, 2023